Laboratori Nazionali di Frascati

LNF-61/48 (1. 9. 61)

R. Gatto: ON THE EXPERIMENTAL POSSIBILITIES WITH COLLIDING BEAMS OF ELECTRONS AND POSITRONS.

Laboratori Nazionali di Frascati del C.N.E.N.
Servizio Documentazione

Nota Interna: N. 91
1 Settembre 1961

R. GATTO: ON THE EXPERIMENTAL POSSIBILITIES WITH COLLIDING BEAMS OF ELECTRONS AND POSITRONS.

ON THE EXPERIMENTAL POSSIBILITIES WITH COLLIDING BEAMS OF ELECTRONS AND POSITRONS.

R. Gatto

Laboratori Nazionali del C.N.E.N. - Frascati - Roma.

I. Introduction

Electron-electron colliding beams were first proposed at Stanford by Barber, Gittelman, O'Neill, Panofsky and Richter[1]. Two separate projects of electron-positron storage rings are presently under development in Frascati. The first project (called AdA, from the Italian "anello di accumulazione"), is already at an advanced stage and it is intended to obtain colliding beams of electrons and positrons of 250 MeV (500 MeV total center-of-mass energy)[2]. The second project (called Adone, which in Italian means "big AdA") should produce beams of much higher energy, possibly up to 1.5 BeV (3 BeV total c.m energy), if this will be shown to be technically feasible[3].

The Stanford electron-electron colliding beam project was mainly designed for the purpose of testing the validity of quantum electrodynamics at small distances by accurate measurements of electron-electron scattering. Electron-positron colliding beams seem. to offer a wider range of experimental possibilities.

In this paper I shall try to present a summary of the high energy physics programs connected with AdA and Adone, and in general with high energy electron-positron storage rings. I hope it will appear from such a summary how the realization of electron-positron storage rings would be relevant to solve a large number of fundamental problems in elementary particle physics.

I shall summarize some of the most important experimental possibilities with electron-positron colliding beams. We shall mainly deal with the following topics:

1) Possible tests of the validity of quantum electrodynamics;
2) Production of strong interacting particles and study of the electromagnetic form-factors for time-like momentum transfer.
3) Investigations of possible resonance and bound states.
4) Production of the suggested vector mesons.
5) Study of some aspects of weak interactions.
6) Verification of the role of strong interacting particles in electrodynamics.

The points I shall discuss do not exhaust the field of experimental investigation made possible by electron-positron colliding beams. Furthermore, at a later stage of development of high energy physics, some new problems may arise that may change in part the picture as presented here.

II. Possible tests of the validity of quantum electrodynamics.

1. I shall be concerned here with the reactions

$$e^+ + e^- \longrightarrow \gamma + \gamma \qquad (1)$$

$$e^+ + e^- \longrightarrow e^+ + e^- \qquad (2)$$

$$e^+ + e^- \longrightarrow \mu^+ + \mu^- \qquad (3)$$

Of these reactions the last one can be used to obtain information on the muon structure. According to the conclusions of the g-2 experiment[5] a possible radius of the muon must be less than 0.4 fermi (1 fermi = 10^{-13} cm). Also, from the same experiment, it is concluded that quantum electrodynamics is valid to distances ~ 0.7 fermi.

Higher order reactions such as

$$e^+ + e^- \longrightarrow \gamma + \gamma + \gamma \qquad (4)$$

$$e^+ + e^- \longrightarrow e^+ + e^- + \gamma \qquad (5)$$

$$e^+ + e^- \longrightarrow \mu^+ + \mu^- + \gamma \qquad (6)$$

may also be conveniently used to test quantum electrodynamics, but their rates are smaller. It should explicitly be mentioned that it is very hard to distinguish experimentally a particular reaction from the corresponding reaction with one more γ emitted.

Thus, for instance, when measuring (1) a relevant fraction of the total rate of (4) will also be included together with the rate of (1). This happens to be especially true at high energies. For instance, at high energy, the cross section for (1) tends to concentrate all forward and backward in the c.m. system and the same happens for reaction (4). A measurement of the gammas from (1) will also include most of the gammas from (4), at least with the currently employed detectors of limited energy resolution. In designing any accurate experiment (as needed for instance to test quantum electrodynamics) the contribution to the number of counts that is due to the competitive reaction, with one more gamma emitted, should explicitily be evaluated for the particular detection system that is used in the experiment. This amount must be calculated together with the modification to the lowest order cross-section formula arising from the so-called radiative corrections, which is of the same order in the electromagnetic coupling constant. All this can be done almost exactly from known formulae of quantum electrodynamics, and what is only required to know is the exact specification of the detection apparatus (including angular and energy resolution) for the particular experiment. An example an how such corrections are calculated can be found in references 4 and 6. It is generally possible to compute them with an error less than 2%. As a matter of language, in the following, when we shall refer to radiative corrections we shall intend all the corrections to the lowest order cross section.

There is a conventional way[7] to discuss the consequency of a breakdown of quantum electrodynamics by introducing in the electrodynamic formulae suitable form factors, that can be thought of as originating from modifications to the electron vertex (smoothing of the charge distribution) or from modifications to the photon propagator. We shall follow this habit in the following in discussing the particular reactions.

2. $e^+ + e^- \longrightarrow \gamma + \gamma$

There are two graphs contributing to

$$e^+ + e^- \longrightarrow \gamma + \gamma$$

(see fig. 1). The modified electron vertex is denoted in fig.1 by a circle, and the modified electron propagator by a black rectangle. In the first graph the virtual electron propagates with a four-momentum $q_1 = p_1 - k_1$, in the second graph with a momentum $q_2 = p_1 - k_2$. (The definitions of the momenta are indicated on the graphs). Both q_1, and q_2 are spacelike four vectors: in the c.m. system

$$q_1^2 = 4E^2 \sin^2 \frac{\vartheta}{2} \qquad (7)$$

$$q_2^2 = 4E^2 \cos^2 \frac{\vartheta}{2} \qquad (7')$$

where E is the energy of one of the incident particles and ϑ is the production angle.

The cross-section formula in the relativistic limit modified to account for a possible break-down of quantum electrodynamics, is, for angle $\vartheta \gg \left(\frac{m_e}{E}\right)$,

$$\frac{d\sigma}{d(\cos\vartheta)} = (\pi r_0^2)\left(\frac{m_e}{E}\right)^2 \frac{|F(q_1^2)|^2 \cos^4\frac{\vartheta}{2} + |F(q_2^2)|^2 \sin^4\frac{\vartheta}{2}}{\sin^2\vartheta} \qquad (8)$$

where r_0 is the electron radius (πr_0^2 is 24.94×10^{-25} cm^2), m_e is the electron mass, and $F(q^2)$ is a form factor depending on the transferred four-momentum squared, q^2; i.e., q_1^2 for the first graph in fig. 1, and q_2^2 for the second graph.

As we have explained, $F(q^2)$ can be thought of as a product $V_e^2(q^2)\, P_e(q^2)$ where $V_e(q^2)$ is a form factor in the electron vertex and $P_e(q^2)$ is a form factor in the electron propagator.

For $F(q^2) = 1$, as in the case of no break-down, Eq (8) reduces to

$$\frac{d\sigma}{d(\cos\theta)} = (\pi r_0^2)\left(\frac{m_e}{E}\right)^2 \frac{1}{2}\,\frac{2-\sin^2\theta}{\sin^2\theta} \tag{9}$$

the usual formula for 2 γ annihilation in flight in the relativistic limit. Eq (9) holds for $\theta \gg \frac{m_e}{E}$. For θ near 0°

$$\frac{d\sigma}{d(\cos\theta)} = (\pi r_0^2)\left(\frac{m_e}{E}\right)^2 \frac{1}{\sin^2\theta + \left(\frac{m_e}{E}\right)^2\cos^2\theta} \tag{10}$$

The total cross section, always in the relativistic limit, is

$$\sigma = (\pi r_0^2)\left(\frac{m_e}{E}\right)^2\left(\log\frac{2E}{m_e} - \frac{1}{2}\right) \tag{11}$$

The differential cross-section at various energies is reported in fig. 2. The total cross-section is given in fig. 3. All these graphs are valid if there is no breakdown.

To estimate the effect of a breakdown we assume for $F(q^2)$ a form

$$F(q^2) = \frac{1}{1+\frac{q^2}{Q^2}} \tag{12}$$

With an energy E = 250 MeV and for Q = 1 GeV, corresponding to a distance of 0.2 fermi, one then expects, according to (8), a relative decrease of the cross section of 12% at 90°, of 7% at 60°, of 4% at 45°, and only of 0.7% at 30°. Thus, already at 250 MeV, if one could carry on an experiment at 60°-90° that can distinguish a 7-10% effect, one can test electrodynamics to distances $\sim$ 0.2 fermi. As the whole effect depends on $(\varepsilon/Q)^2$, at least in this model, on would also roughly expect that a similar experiment at 500 MeV would test electrodynamics to distances $\sim$ 0.1 fermi.

The radiative corrections at 90° are roughly of the same order as the effects we are discussing. For instance with an isotropic (in c.m.) upper limit for the energy of the additional photon of, say 5 MeV, one finds at 90° a decrease of 14% of the cross section at 250 MeV and of 20% at 500 MeV. These figures will however be substantially changed when a more realistic, necessarily non-isotropic, upper limit will be considered, as defined directly from the particular detection system employed. Such computation is being carried out in Frascati for particular specifications of the detection system[8].

3. $e^+ + e^- \to e^+ + e^-$

We shall next consider the reaction

$$e^+ + e^- \longrightarrow e^+ + e^-$$

The Feynman graphs are reported in fig. 4. Here the white rectangle denotes the modified photon propagator. The transferred four-momentum is q_1 in the first graph and k in the second graph: q_1 is space-like, k is time-like. In the c.m. system

$$q_1^2 = 4E^2 \sin^2 \frac{\theta}{2} \tag{13}$$

$$k^2 = -4E^2 \tag{13'}$$

where θ is the c.m. scattering angle.

The cross section formula in the relativistic limit, with a form factor, F, to account for a possible break-down of quantum electrodynamics, is, for finite angles

$$\frac{d\sigma}{d(\cos\theta)} = (\pi r_0^2)\left(\frac{m_e}{E}\right)^2 \left\{ \frac{1}{4} \frac{1+\cos^4\frac{\theta}{2}}{\sin^4\frac{\theta}{2}} |F(q_1^2)|^2 - \right.$$

$$- \frac{1}{2} \frac{\cos^4\frac{\theta}{2}}{\sin^2\frac{\theta}{2}} \mathrm{Re}\left[F(q_1^2) F(k^2)^*\right] + \tag{14}$$

$$\left. + \frac{1}{8}(1+\cos^2\theta)|F(k^2)|^2 \right\}$$

This time the form factor F can be thought of as a product $V_e^2 P_\gamma$ where V_e is the form factor for the electron and P_γ that for the photon propagator. Strictly speaking, the form factor V_e in this process does not need to be the same one occurring in $e^+ + e^- \rightarrow 2\gamma$, since here both electrons are real while in that case one of them was virtual. Therefore they should strictly be considered as different quantities.

With $F = 1$ one obtains from (14) the well known Bhabha formula. Graphs of the differential cross section are given in fig. 5 for different energies E of the incident electron in c.m.

To the purpose of having same indication, we shall estimate the effect of a breakdown by inserting in (14) a particular form of $F(q^2)$. We can use the same form as in (12). Note that the form factor appears in (14) taken at two different values, one spacelike, one timelike. In fig. 6 we have reported the relative correction to the differential cross section for $e^+ + e^- \rightarrow e^+ + e^-$ as computed from (14) with a form factor of the form (12) for two different values of the breakdown parameter Q. The value $Q^{-1} = 0.1$ fermi corresponds to a cut-off energy ~ 2 GeV and the value $Q^{-1} = 0.3$ fermi to an energy ~ 670 MeV. The percentage effect of the breakdown (reported in fig. 6) is computed with respect to the cross-section obtained from (14) by putting $F = 1$. One sees from fig. 6 that an appreciable effect of the order of 10% requires an energy larger than about 300 MeV if $Q^{-1} = 0.1$ fermi, or an energy larger than 100 MeV if $Q^{-1} = 0.3$ fermi. With our choice of (12) the break-down effect acts in the direction of reducing the cross-section.

The maximum effect is expected to be visible, if it exists of course, mainly around 90°. Note also that the form factor $F(t_1^2)$ is less than 1 with our choice (12), but $F(k^2)$ is greater than 1, because k^2 is time-like. However the net effect results in a decrease of the cross section. It should however be stressed that all these considerations are completely model dependent. Furthermore radiative corrections must be computed, once the detection apparatus has been designed.

4. $e^+ + e^- \rightarrow \mu^+ + \mu^-$

Finally we consider the reaction

$$e^+ + e^- \rightarrow \mu^+ + \mu^-$$

The relevant Feynman graph is reported in fig. 7. The black circle indicates the muon vertex. The transferred four-momentum is $k = p_1 + p_2$ and it is time-like. In the c.m. system

$$k^2 = -4E^2$$

The cross-section formula is, always in the c.m. system,

$$\frac{d\sigma}{d(\cos\theta)} = \frac{\pi}{4}\alpha^2\lambda^2\beta_\mu\left[\frac{1}{2}(1+\cos^2\theta) + \frac{1}{2}\left(\frac{m}{E}\right)^2\sin^2\theta\right]|F(k^2)|^2 \qquad (15)$$

In (15) $\alpha = 1/137$, λ is the reduced wavelength of the incoming electron or positron, β_μ is the velocity of the emitted muon, and m is the muon mass. The form factor F appears as a multiplicative factor in the form $|F(k^2)|^2 = |F(-4E^2)|^2$. This form factor can be thought of as a product V_μ, V_e, P_γ, of the form factors modifying the muon and electron vertex and the photon propagator.

The differential cross-section for $e^+ + e^- \rightarrow \mu^+ + \mu^-$ in c.m. is reported in fig. 8. The angular dependence of the cross-section does not depend on a possible break-down of electrodynamics or on a muon form factor.

The total cross-section can be written as a function of x = E/m. It is given by

$$\sigma = 2.18 \times 10^{-32}\ \text{cm}^2\ \frac{1}{x^2}\left(1-\frac{1}{x^2}\right)^{\frac{1}{2}}\left(1+\frac{1}{2x^2}\right)|F(-4E^2)|^2 \qquad (16)$$

A graph of the cross-section (16), for $F = 1$ versus $x = E/m$ can be found in fig. 9. On the same figure are reported, for purpose of comparison, the "perturbation theory" cross sections for $e^+ + e^- \to \pi^+ + \pi^-$, $e^+ + e^- \to p + \bar{p}$, and $e^+ + e^- \to K + \bar{K}$ also as functions of the dimension less parameter $x = E/M$, where M is the mass of the produced particle ($M = m_\mu, m_\pi, m_p$ and m_K respectively).

As we have said a break-down can only be felt in the total cross-section, but not in the relative angular distribution. With a form factor of the type (12) one expects a 10% relative increase of the total cross-section already at an energy $E \sim 300$ MeV if $Q^{-1} = 0.1$ fermi, or at an energy as small as 100 MeV if $Q^{-1} = 0.3$ fermi. The effect is in the direction of increasing the cross-section because of the timelike argument of F, at leact in the realm of the simple model considered.

Radiative corrections are due mainly to the infrared terms and to the photon emission by the incident electrons, mainly along their direction of flight. A precise estimate requires a specification of the detection apparatus. With a (very unrealistic) isotropic cut-off in c.m. for the maximum photon energy of 5 MeV, one finds large corrections in the total cross section of the order $\sim$ 10% at 100 MeV, 20% at 300 MeV.

III. Annihilation into strong interacting particles.

1. Annihilation into strong interacting particles is described at lowest electromagnetic order (order of e^4 in the intensity), by the graph of fig. 10. The virtual photon four momentum is $k = p_1 + p_2$ and it is timelike.

In the c.m. system $k^2 = -4E^2$. One can show from gauge invariance that the final particles produced according to the graph in fig. 10, must be in a state of total angular momentum $J = 1$ and total parity $P = -1$. Moreover the charge conjugation quantum number for the final state must be $C = -1$ and the total isotopic spin T can be 0 or 1.

At the next electromagnetic order (order of e^6) one has to include terms of interference between the lowest order graph of fig. 10 and graphs with two virtual photons and also terms giving the contribution from undetectable bremsstrahlung processes. Of all such terms, those originating from the interference between the lowest order graph and a graph in which two photons are exchanged between the electron line and the final particles violate the selection rules that we have listed. It can be easily seen however that in any experiment that treats charges symmetrically (such as a total cross-section, or, for instance, $e^+ + e^- \to \pi^+ + \pi^-$ at a definite angle, but without distinguishing the charges) such terms don't contribute. Therefore, for such experiments we can safely apply, to the order e^6 in the probabilities, the selection rules, $J = 1$, $P = -1$, $C = -1$, $T = 0,1$.

We shall also say, is this case, that the reaction goes through the "one-photon channel". In the following without need of specification, all our considerations are limited to the "one-photon channel", and thus they are valid to the order of e^6 for charge-symmetric experiments -- quite satisfactory for the expected experimental accuracy.

2. $e^+ + e^- \to$ pions [3]

The pions produced in

$$e^+ + e^- \to n \text{ pions} \tag{17}$$

must be in a state with $J=1$, $P=-1$, $C=-1$, and $T=1$ for n even, $T=0$ for n odd. In particular they cannot all be neutral. The cross-section for

$$e^+ + e^- \to \pi^+ + \pi^- \tag{18}$$

in c.m. is given by

$$\frac{d\sigma}{d(\cos\theta)} = \frac{\pi}{16}\alpha^2 \lambda^2 \beta_\pi^3 |F(k^2)|^2 \sin^2\theta \tag{19}$$

where, as before, λ is the reduced wavelength of the incoming electron, β_π is the velocity of the final pion and $F(k^2)$ is the pion electromagnetic form-factor.

The total cross-section is

$$\sigma = \frac{1}{m_\pi^2}(0.54 \times 10^{-32} \text{ cm}^2)\frac{1}{x^2}\left(1-\frac{1}{x^2}\right)^{\frac{3}{2}} |F(-4E^2)|^2 \tag{20}$$

and for $F=1$ is reported in fig. 9, as a function of E/m_π.

However $F(-4E^2)$ is almost certainly quite different from 1. With the resonant form proposed for F by Frazer and Fulco [10] the cross section at E = 230 MeV reaches a value of $\sigma = 8.35 \times 10^{-31}$ cm^2. With the form proposed by Bowcock, Cottingham, and Lauriè [11] at E = 330 MeV it reaches a value $\sigma = 6.6 \times 10^{-31}$ cm^2 (in the first case 17 times larger than perturbation theory, in the second case 33 times larger).

In

$$e^+ + e^- \rightarrow \pi^+ + \pi^- + \pi^0$$

the relative $\pi^+ - \pi^-$ angular momentum ℓ, and the π^0 angular momentum relative to $\pi^+ - \pi^-$ must satisfy $\ell = L = 1,3,5$ etc. The cross-section in c.m. is

$$\frac{d\sigma}{d\omega_+ d\omega_- d(\cos\theta)} = \frac{\alpha}{(2\pi)^2} \frac{\lambda^2}{64} |H|^2 \sin^2\theta \, (\vec{p}_+ \times \vec{p}_-)^2 \qquad (21)$$

where ω^+, ω^- are the energies of $\pi^+ \pi^-$, $\vec{p}_+, \vec{p}_-$ their momenta, θ is the angle between the normal to the production plane and the incident electron direction, and H is a form factor.

The form factors F (Eq. 13) and H (Eq 21) are essential for the theory of nucleon structure.

3. K mesons.

Eq (19) applies to

$$e^+ + e^- \longrightarrow K^+ + K^-$$
$$\longrightarrow K^0 + \bar{K}^0$$

provided F is the K-meson form factor. From C invariance we find that the final amplitude for neutral K production must be of the form

$$K_1^0 K_2^0 - K_2^0 K_1^0 \qquad (22)$$

Thus no $K_1^0 K_1^0$ or $K_2^0 K_2^0$ pairs are produced. Note that, as long as the K_1^0, K_2^0 propagate in vacuum, (22) conserves its form at any time [the time dependences are $K_1^0 \to K_1^0 e^{-(\lambda_1 + im_1)t}$, $K_2^0 \to K_2^0 e^{-(\lambda_2 + im_2)t}$ where λ are the inverse decay times and m the masses of K_1^0 and K_2^0].

4. $e^+ + e^- \rightarrow \pi^0 + \gamma$ (12) and $e^+ + e^- \rightarrow e^+ + e^- + \pi^0$ (13)

The reaction

$$e^+ + e^- \rightarrow \pi^0 + \gamma$$

is of great theoretical interest because one measures through it the form factor for $\pi^0 \rightarrow \gamma + \gamma$. Moreover it may have a very large peak if there is a vector meson (as for instance suggested by Nambu[14]) that decays into $\pi^0 + \gamma$. Its cross section in c.m. is given by

$$\frac{d\sigma}{d(\cos\theta)} = \frac{\pi\alpha}{m_\pi^3} \frac{1}{\tau} \beta_\pi^3 (1 + \cos^2\phi) \left| \frac{G(-k^2)}{G(0)} \right|^2 \qquad (23)$$

where β_π is the π^0 velocity, $\cos\phi$ the production angle, τ is the π^0 lifetime and $G(-k^2)$ is the form factor of $\pi^0 \rightarrow \gamma + \gamma$.

For different values of k^2 this same form factor appears in various phenomena. For $k^2 = 0$ it determines the rate of π^0 decay

$$\frac{1}{\tau} = \frac{m_\pi^3}{64\pi} |G(0)|^2 \qquad (24)$$

For $k^2 > 0$ (spacelike) if determines the rate of the Primakoff effect[15] ($\gamma \rightarrow \pi^0$ in the Coulomb field of a nucleus). For $-m_\pi^2 < k^2 < 0$ it gives the rate for Dalitz pairs ($\pi^0 \rightarrow \gamma + e^+ + e^-$). For $k^2 < -m_\pi^2$ it determines the cross-section (23).

J = 1 pion-pion resonances with T=1 or with T=0 would both produce peaks in $G(k^2) = G(-4E^2)$ at the relevant E.

The total cross section from (23) is (we take $\tau = 2.2 \times 10^{-16}$ sec)

$$\sigma = 2.75 \times 10^{-35} \text{ cm}^2 \left| \frac{G(-k^2)}{G(0)} \right|^2 \left(1 - \frac{1}{4} x^{-2}\right)^{3/2} \qquad (25)$$

with $x = E/m_\pi$. With $G = 1$ the cross section rises from zero to the small constant value of 2.75×10^{-35} cm^2. However if there is a vector meson with $T=0$ $J=1$ decayng into $\pi^0 + \gamma$, as repeatedly suggested, the cross section for $e^+ + e^- \to \pi^0 + \gamma$ would have a very sharp peak at a total c.m. energy equal to the mass M of the vector meson. The measured cross-section would be the average

$$\bar{\sigma} = \frac{1}{\Delta E} \int_{E=\frac{1}{2}(M-\Delta E)}^{E=\frac{1}{2}(M+\Delta E)} \sigma \, dE \qquad (26)$$

if ΔE is the experimental energy resolution. If we use a Breit-Wigner formula for σ, assume $M \leq 3m_\pi$ and a resonable branching ratio for decay of the vector meson into $e^+ + e^-$, of the order of 10^{-3}, we find

$$\bar{\sigma} = 1.3 \times 10^{-28} \left(\frac{\Gamma}{2\Delta E}\right)^2 \text{cm}^2 \qquad (27)$$

where Γ is the decay rate of the vector meson. With $\Gamma \sim 10^{20}$ sec^{-1} we find $\bar{\sigma} = 0.8 \times 10^{-29}$ $(2\Delta E$ in MeV$)^{-1}$ cm^2 (a value about 10^5 times bigger than "perturbation theory" for $\Delta E \sim$ ~ 10 MeV.

Independently of the existence of the hypothetical vector meson, the generally accepted $T=1$, $J=1$ pion-pion resonance would produce a peak in the cross section. With the Frazer-Fulco parameters[10] the peak would be around E = 240 MeV, with a maximum cross-section of the order of 0.4×10^{-33} cm^2. With the Bowcock-Cottingham-Lauriè parameters[11] the peak would be around E = 340 MeV and the maximum cross-section of the order 0.8×10^{-33} cm^2.

A more refined theory can be given where both resonances ($T=0$ and $T=1$) are considered [16], but it will not be reported here.

In measuring $e^+ + e^- \to \pi^0 + \gamma$ one has to discriminate against $e^+ + e^- \to \gamma + \gamma + \gamma$. This should be possible on account of the different angular distributions.

The reaction $e^+ + e^- \to e^+ + e^- + \pi^0$ has a large cross-section $\sim 2.2\times10^{-35}$ cm^2 ϵ/m_π if one takes a value of $\tau = 2.2\times10^{-16}$ sec for the π^0 lifetime.

5. The cases examined above of big effects produced by $J=1$ pion-pion resonance are particular cases of a more general situation. It can be shown[12] by an application of charge conjugation and angular momentum selection rules, and by estimates of the order of magnitudes, that $e^+ - e^-$ collisions will in general be very sensitive to intermediate resonant states with $J=1$, $C=-1$, (and of course, with zero nucleonic number and zero strangeness). Resonances with other quantum numbers will generally escape detection.

6. $e^+ + e^- \longrightarrow$ (baryon) + (anti-baryon) (12)

The final baryons

$$e^+ + e^- \longrightarrow p + \bar{p},\ n + \bar{n}$$
$$\longrightarrow \Lambda + \bar{\Lambda}$$
$$\longrightarrow \Sigma + \bar{\Sigma}$$
$$\longrightarrow \Xi + \bar{\Xi}$$

are produced in $^3S_1$ and $^3D_1$. Therefore near threshold σ is isotropic and proportional to the final β. The differential cross section in c.m. is

$$\frac{d\sigma}{d(\cos\theta)} = \frac{\pi}{8}\alpha^2\lambda^2\beta\left[\left|F_1(k^2) + \mu F_2(k^2)\right|^2(1+\cos^2\theta) + \right. \tag{28}$$
$$\left. + \left|\frac{m}{E}F_1(k^2) + \frac{E}{m}\mu F_2(k^2)\right|^2\sin^2\theta\right]$$

where: m is the baryon mass; $F_1(k^2)$ and $F_2(k^2)$ are analytic continuations of the electric and magnetic form factors of the baryon for $k^2 < -4m^2$; μ is the static anomalous magnetic moment of the baryon. The normalization is $eF_1(0)$ = charge of the baryon, $F_2(0) = 1$.

With $F_1 = 1$, $F_2 = 0$

$$\sigma = m^{-2}(2.1 \times 10^{-32}\ \text{cm}^2)\frac{1}{x^2}\left(1 - \frac{1}{x^2}\right)^{\frac{1}{2}}\left(1 + \frac{1}{2}\frac{1}{x^2}\right) \tag{29}$$

with m in BeV and x = E/m. For $e^+ + e^- \to p + \bar{p}$ this " perturbation theory" cross section is reported in fig. 9. The value (29) may serve as an indication in the lack of anything better, but it might very well be completely different from the actual cross-section.

In the region $k^2 = -4\epsilon^2 < -4m^2$, where the form factors are explored through (28), they are generally complex. This leads to the existence of a polarization $P(\theta)$ of the produced baryon along the normal to the production plane given by

$$\frac{d\sigma}{d(\cos\theta)} P(\theta) = -\frac{\pi}{8}\alpha^2\lambda^2\beta^3\mu\frac{\epsilon}{m} Im\left[F_1(k^2)F_2^*(k^2)\right]\sin(2\theta) \qquad (30)$$

For the antibaryon the polarization is opposite.

A different reaction is

$$e^+ + e^- \rightarrow \Sigma^+ + \bar{\Lambda}^0 \quad or \quad \Lambda^0 + \bar{\Sigma}^0$$

It proceeds to $^3S_1$ and $^3D_1$ for relative Σ-Λ parity even (σ proportional to β and isotropic); to $^1P_1$ and $^3P_1$ for parity odd (σ proportional to β^3 and with a $\cos^2\theta$ term). It is therefore very sensitive to the relative Σ-Λ parity.

IV. Annihilation into pairs of vector mesons. Weak interactions.

1. Vector mesons have been proposed in the theory of strong interactions, from a principle of "localized gauge invariance",[17] and also in the theory of weak interactions to act as intermediaty agents of the weak couplings[18]. Pairs of vector mesons can be produced according to

$$e^+ + e^- \to B + \bar{B}$$

where B is the vector meson.

From the selection rules of section III-1 one finds that the possible final states are $^1P_1$, $^5P_1$ and $^5F_1$. Thus near threshold one expects a β^3 dependence (β =velocity the of the B meson in c.m.).

For the differential cross-section in c.m. one can write

$$\frac{d\sigma}{d(\cos\theta)} = \frac{\pi}{16}\alpha^2\lambda^2\beta^3\Big\{2\Big(\frac{E}{m_B}\Big)^2\Big|G_1(k^2)+\mu G_2(k^2)+\tfrac{1}{4}\epsilon G_3(k^2)\Big|^2(1+\cos^2\theta)+$$

$$+\sin^2\theta\Big[2\Big|G_1(k^2)+2\Big(\frac{E}{m_B}\Big)^2 G_3(k^2)\Big|^2+ \qquad (31)$$

$$+\Big|G_1(k^2)+2\Big(\frac{E}{m_B}\Big)^2\mu G_2(k^2)\Big|^2\Big]\Big\}$$

where G_1, G_2 and G_3 are form factors, and $\mu+\epsilon$ and $\frac{1}{4}\epsilon$ are the possible static anomalous magnetic moment and quadrupole moment of B. The normalization is $e\,G_1(0)$ = charge of , and $G_2(0) = G_3(0) = 1$.

With $G_1 = 1$ and $G_2 = G_3 = 0$ the total cross-section is

$$\sigma = m_B^{-2}(2.1 \times 10^{-32} cm^2) \frac{3}{4}\left(1 - \frac{1}{x^2}\right)^{\frac{3}{2}}\left(\frac{4}{3} + \frac{1}{x^2}\right) \qquad (32)$$

with m_B in BeV and $x = E/m_B$.

Graphs (32) for various values of m_B are reported in fig. 11. In figures 12, 13 and 14 are reported graphs of the total cross-sections, as obtained from (31) for constant form factors and with inclusion of anomalous magnetic dipole or electric quadrupole moments. One sees that electron-positron collisions are a very effective mean for producing possible unstable vector mesons. The angular dependences of the cross-section are illustrated in the figures 15, 16, 17 and 18.

One sees from the figures that both the total cross sections and the differential cross-sections are generally very sensitive to anomalous moments.

Also, when B decays, the decay products will exhibit specific angular distributions reminiscent of the polarization state of B (since B has spin one, even simple alignment produces anisotropic distributions of the secondaries). These distributions have been calculated but will not be discussed here[16].

The cross section (32) violates unitarity at high energy. One can show[16] that, for the one photon channel that we are discussing, unitarity puts an upper limit of

$$\frac{3}{4}\pi\lambda^2$$

to the total reactions cross-section at energy $E = 4/\lambda$.

The cross section (32) instead tends to the constant value of $m_\beta^{-2}(2.1\times10^{-32}\ \mathrm{cm}^2)$ at large E. If anomalous moments are kept, with constant form factors, the cross section even increases with energy. However with (32) the violation of unitarity only occurs at energies of the order of $10^2\, m_\beta$ (or $\chi \cong 10^2$). So one can hope that for small χ the cross-sections given above are still valid.

2. The considerationsof the last section apply in particular to the production of the semi-weak interacting vector mesons, proposed for the theory of weak interactions. Note that the production of such mesons from e^+ e^- collisions is perhaps one of the best ways one can think of for producing vector mesons. In fact any process with competive strong interactions would mask under a big background the production of semi-weak vector mesons (necessarily of electromagnetic or of semiweak strength).

For the rest, weak interactions are not expected to play a significant role in electron-positron collisions, at least up to energies of the order of 30 BeV. At such energies weak interactions could be felt through their interference with electromagnetic interactions and one could find for instance a longitudinal polarization of the muons produced in $e^+ + e^- \longrightarrow \mu^+ + \mu^-$ (if there are weak neutral lepton currents, etc.).

A semiweak-interacting neutral vector meson B° cannot be coupled to leptons if it is also coupled to the weak neutral strangeness-conserving current. If B° exists and it is coupled to leptons one would have a resonant contribution form

$$e^+ + e^- \longrightarrow B^\circ \longrightarrow \mu^+ + \mu^-$$

Such a contribution might be very big indeed. With reasonable values of the parameters one could well have a contribution from the resonance about three times bigger than the electromagnetic cross-section for $e^+ + e^- \to \mu^+ + \mu^-$.

V. Possibility of measuring the role of virtual strong interacting particles in electromagnetic interactions.

Any experimental investigation about the limits of validity of quantum electrodynamics will eventually run into the difficulty of having to deal with effects of the same order as the effects originating from virtual strong interacting particles. These last effects must certainly exist and because of the present difficulties in treating weak interactions their exact evaluation will probably remain uncertain.

Effects from virtual strong interactions are still unimportant at energies E of a few hundreds of a MeV where they can change the cross-section only by some percent. However at higher energies they will become important. It is then relevant to note that direct measurements of the production of strong interacting particles in electron-positron collisions can be directly related to the quantities that express the effect of virtual strong interacting particles on the electrodynamic parameters. Thus, the modification to the photon propagator can be expressed by a certain function, $\pi(k^2)$, known to the electrodynamicists, and which is additive with respect to the contribution from the various virtual states. There is thus a part of $\pi(k^2)$, call it $\pi_\pi(k^2)$, which comes, for instance, from the presence of virtual pions. Now, one can show[16] that (excluding higher order corrections)

$$\pi_\pi(-4\varepsilon^2) = \frac{\varepsilon^2}{\pi^2\alpha}\,\tilde{\sigma}_\pi(\varepsilon)$$

where $\tilde{\sigma}_\pi(\varepsilon)$ is the (directly measurable) total cross section for production of pions in electron positron collisions at a center of mass energy E for incoming electron. The same holds for the other contributions (from K-mesons, etc).

VI. Conclusions.

It is apparent from the variety of applications to problems of fundamental importance in elementary particle physics that high energy colliding beams of electrons and positrons deserve an intensive study and no effort should be spared in my opinion in view of their realization. Electron-positron colliding beams would permit a new, powerful, and direct approach to the solution of long-standing problem of high energy physics, and a concentration of efforts to produce such beams would be highly desirable.

References:

(1) Barber, Gittelman, O'Neill, Panofsky, Richter, HEL-170-Stanford; G.K.O'Neill - Proceedings CERN Conference on high energy accelerators and instrumentation, CERN 1959, Pag. 125; W.K.H. Panofsky, Proceedings of the 1960 Rochester Conference, pag. 769 O'Neill and Woods, Phys. Rev. 115, 659 (1959).

(2) C. Bernardini, G. Corazza, G. Ghigo, B. Touschek, Nuovo Cimento 18, 1293 (1960) - See also the paper by C. Bernardini, U. Bizzarri, G. Corazza, G. Ghigo, R. Querzoli and B. Touschek, presented at this Conference.

(3) F. Amman, C. Bernardini, R. Gatto, G. Ghigo, B. Touschek; Nota interna 69, Frascati Laboratories, January 1961 (unpublished); and paper by Amman and Ritson presented at this Conference.

(4) See (1), and Yung Su Tsai, Phys. Rev. 120, 269, 1960.

(5) Charpak, Farley, Garwin, Muller, Sens, Telegdi, and Zichichi, Physical Review Letters 6, 128, 1961.

(6) J.D. Bjorken, S.D. Drell and S.C. Frautschi, Phys. Rev. 112, 1409, (1958).

(7) S. Drell, Annuals of Physics, 4, 75, 1958.

(8) A. Mosco and G. Putzolu (private communication).

(9) N. Cabibbo and R. Gatto; Phys. Rev. Letters 4, 313, 1960, Exactly the same results are also given in reference (4).

(10) W.R. Frazer and J.R. Fulco, Phys. Rev. 117, 1609, 1960.

(11) Bowcock, Cottingham, and Lauriè, Phys. Rev. Lett. 5, 386 (1960)

(12) N. Cabibbo and R. Gatto, Nuovo Cimento, 20, 185, 1961.

(13) F.E. Low, Phys. Rev. 120, 582 (1960); F. Chilton, Phys. Rev. 123, 656, 1961.

(14) Y. Namba, Phys. Rev. 106, 1366, 1957.

(15) H. Primakoff, Phys. Rev. 81, 899 (1951).

(16) See, for instance, R. Gatto - Proceedings of International Conference on the Theoretical Aspects of Very High Energy Physics, CERN, June 1961 (to be published).

(17) C.N. Yang and R. Mills, Phys. Rev. 96, 191 (1954); J. Sakurai, Annals of Physics, 11, 1, 1960.
A. Salam and J. Ward, Nuovo Cimento, 19, 167 (1961)
M. Gell-Mann (to be published)

(18) R.P. Feynman and M. Gell-Mann, Phys. Rev. 109, 193 (1958)
T.D. Lee and C.N. Yank, Phys. Rev. 119, 1410 (1960).

CAPTION TO FIGURES

Fig. 1: Feynman graphs for $e^+ + e^- \longrightarrow \gamma + \gamma$. The modified electron vertex is represented by a circle and the modified electron propagator by a block rectangle. The momentum transfer is $q_1 = p_1 - k_1$ in the first graph and $q_2 = p_1 - k_2$ in the second graph, and they are both space-like.

Fig. 2: Differential cross-section in c.m. for $e^+ + e^- \longrightarrow \gamma + \gamma$ at 10, 50, 100 and 1000 MeV. incident electron energy on a logarithmic scale. The expression $\left(\frac{1}{\pi r_0^2}\right) \frac{d\sigma}{d(\cos\theta)}$ is plotted $vs\ \theta$ ($\pi r_0^2 = 24.94 \times 10^{-25}$ cm^2). No radiative corrections are included as they depend critically on the particulat experimental apparatus.

Fig. 3: Total cross-section for $e^+ + e^- \longrightarrow 2\gamma$ on a logarithmic scale vs electron energy in c.m.

Fig. 4: Feynman graphs for $e^+ + e^- \longrightarrow e^+ + e^-$. The modified electron vertex is represented by a circle and the modified photon propagator by a rectangle. The momentum transfer is $q_1 = p_1 - p_1'$ in the first graph and $k = p_1 + p_2$ in the second graph: q_1 is space-like, k is timelike.

Fig. 5: Differential cross-section for $e^+ + e^+ \longrightarrow e^+ + e^-$ at various energies of the incident electron in c.m. on a logarithmic scale. No radiative corrections are included.

Fig. 6: Relative correction to the differential cross section for $e^+ + e^- \longrightarrow e^+ + e^-$ arising from the introduction of a form factor $F(q^2) = (1 + q^2/Q^2)^{-1}$ for Q = 2000 MeV and Q = 670 MeV.

Fig. 7: Feynman graph for $e^+ + e^- \longrightarrow \mu^+ + \mu^-$. The modified muon vertex is represented by a black circle. The momentum transfer $k = p_1 + p_2$ is time-like.

Fig. 8: Differential cross section in c.m. for $e^+ + e^- \rightarrow \mu^+ + \mu^-$ for various energies E of the incident electron, normalized to one at 0°.

Fig. 9: Total cross-sections in "perturbation theory" for $e^+ + e^- \longrightarrow \mu^+ + \mu^-, \longrightarrow \pi^+ + \pi^-, \longrightarrow p + \bar{p}, \longrightarrow K + \bar{K}$. The cross sections are plotted vs(E/M) where E is the energy of the impinging electron in c.m. and M the mass of one of the energing particles ($M = m_\mu, m_\pi, m_p, m_K$)

Fig. 10: Feynman graph for $e^+ + e^- \longrightarrow$ strong interacting particles. The momentum transfer $k = p_1 + p_2$ is timelike.

Fig. 11: Total cross section for $e^+ + e^- \longrightarrow$ (pair of spin one mesons) for different values of the mass of the meson, m_B, reported as a function of E/m_B. The form factory are assumed to be constant and no anomalous moments are included.

Fig. 12: Total cross section per $e^+ + e^- \longrightarrow$ (pair of spin one mesons) with constant form factors, anomalous magnetic dipole moment = 1, and no anomalous electric quadrupole moment.

Fig. 13: Total cross section for $e^+ + e^- \longrightarrow$ (pair of spin one mesons) with constant form factors, anomalous magnetic dipole moment -1, and no anomalous electric quadrupole moment.

Fig. 14: Total cross section for $e^+ + e^- \longrightarrow$ (pair on spin one mesons) with constant form factors, anomalous magnetic dipole moment 2, and no anomalous electric quadrupole moment.

Fig. 15: Angular distribution for $e^+ + e^- \longrightarrow$ (pair of spin one mesons) with constant form factors, and no anomalous moments.

Fig. 16: Angular distribution for $e^+ + e^- \longrightarrow$ (pair of spin one mesons) with constant form factors, anomalous magnetic dipole moment +1, and no anomalous electric quadrupole moment.

Fig. 17: Angular distribution for $e^+ + e^- \longrightarrow$ (pair of spin one mesons) with constant form factors, anomalous magnetic dipole moment -1, and no anomalous electric quadrupole moment. The distribution is $\sim \sin^2 \not\theta$, independent of energy.

Fig. 18: Angular distribution for $e^+ + e^- \longrightarrow$ (pair of spin one mesons) with constant form factors, anomalous magnetic dipole moment 2, and no anomalous electric quadrupole moment.

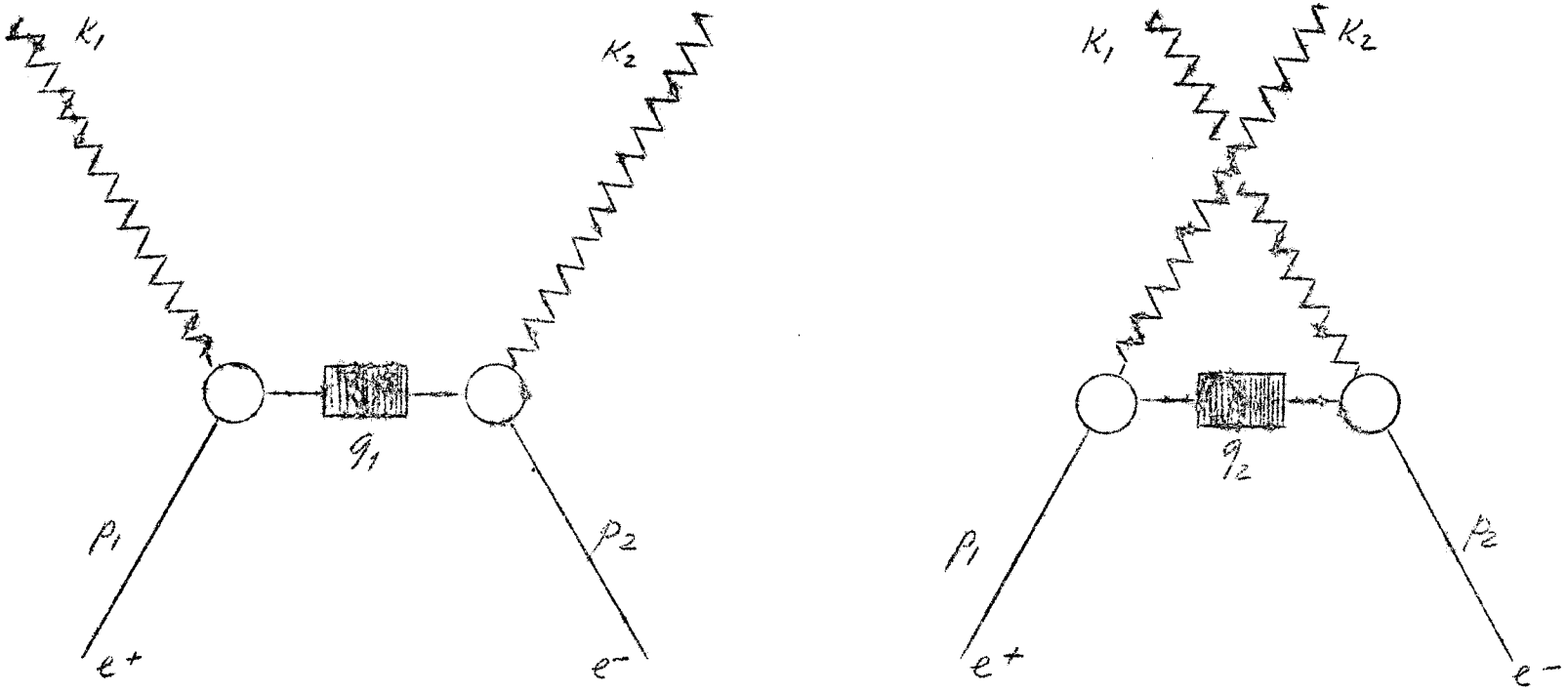

FIG. 1

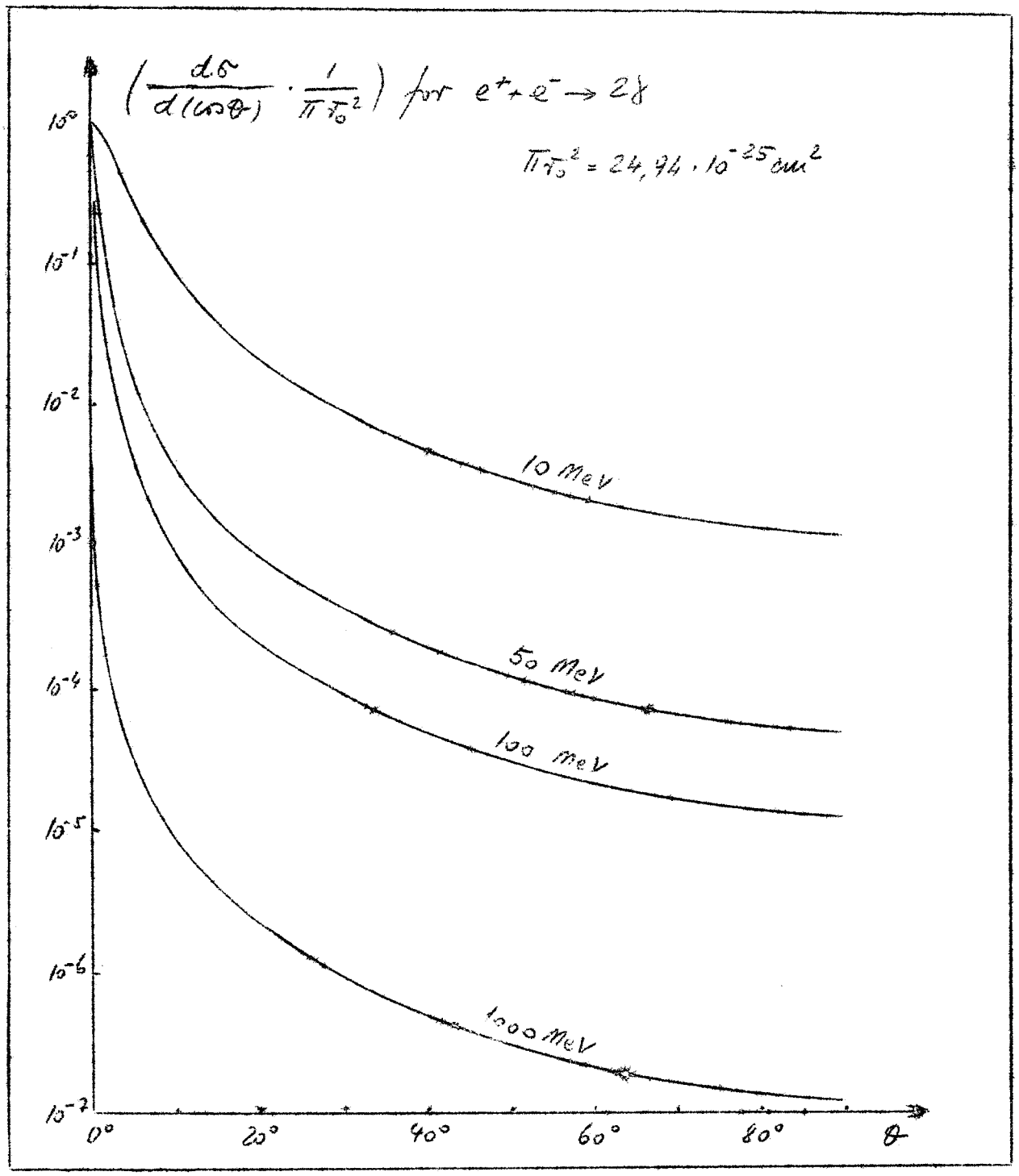
$\left(\frac{d\sigma}{d(\cos\theta)} \cdot \frac{1}{\pi r_0^2}\right)$ for $e^+ + e^- \to 2\gamma$
$\pi r_0^2 = 24,94 \cdot 10^{-25} cm^2$
10^0
10^{-1}
10^{-2}
10^{-3}
10^{-4}
10^{-5}
10^{-6}
10^{-7}
10 MeV
50 MeV
100 MeV
1000 MeV
0°
20°
40°
60°
80°
θ

FIG. 2

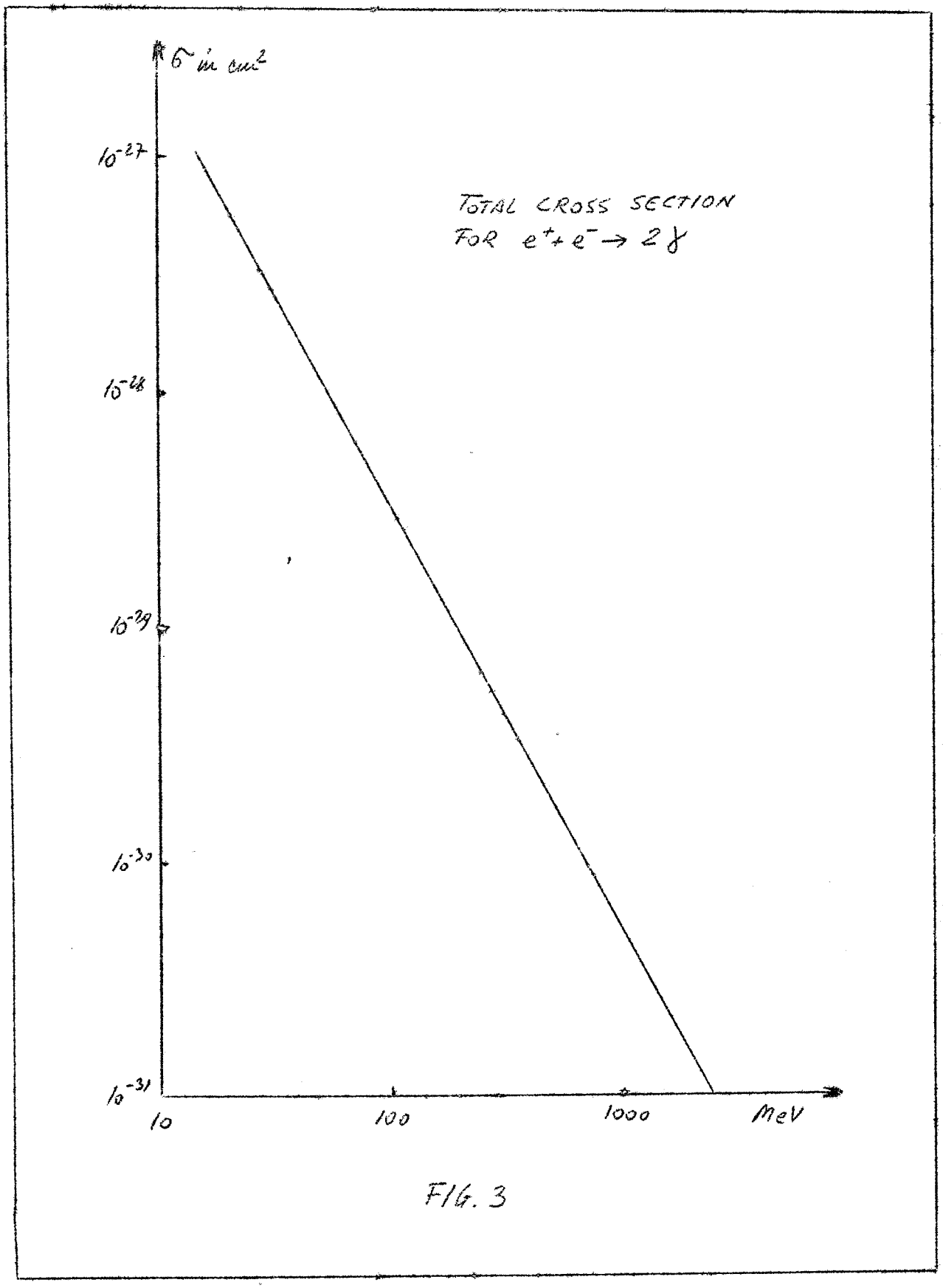
σ in cm²
10⁻²⁷
10⁻²⁸
10⁻²⁹
10⁻³⁰
10⁻³¹
TOTAL CROSS SECTION
FOR e⁺ + e⁻ → 2γ
10
100
1000
MeV

FIG. 3

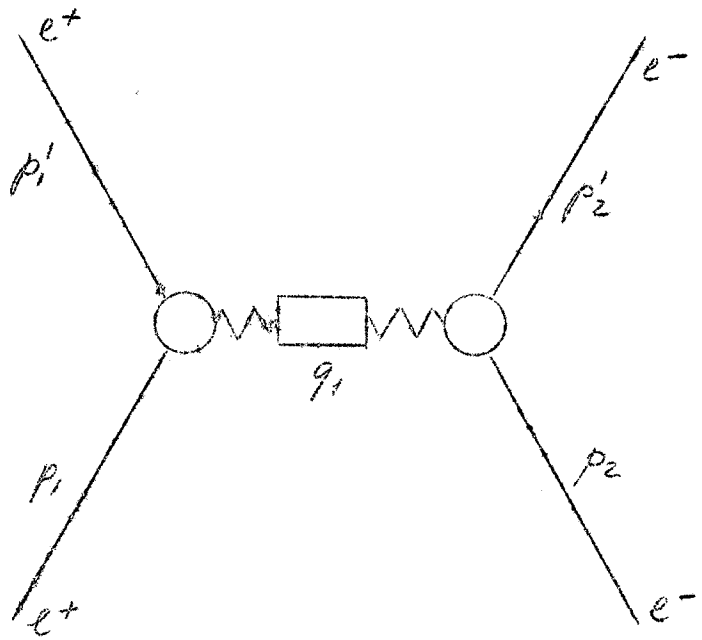

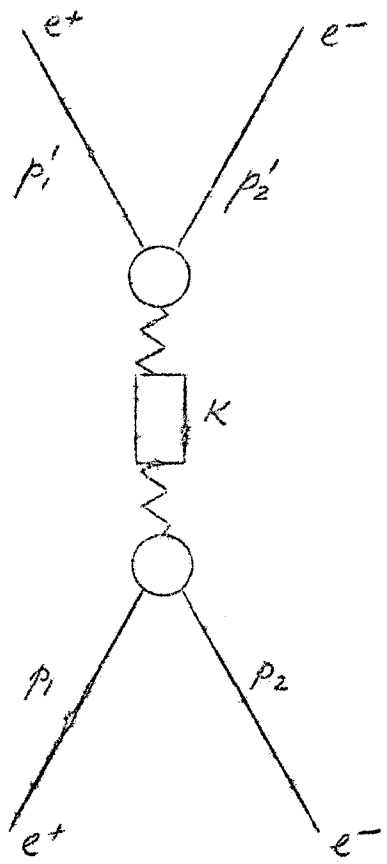

FIG. 4

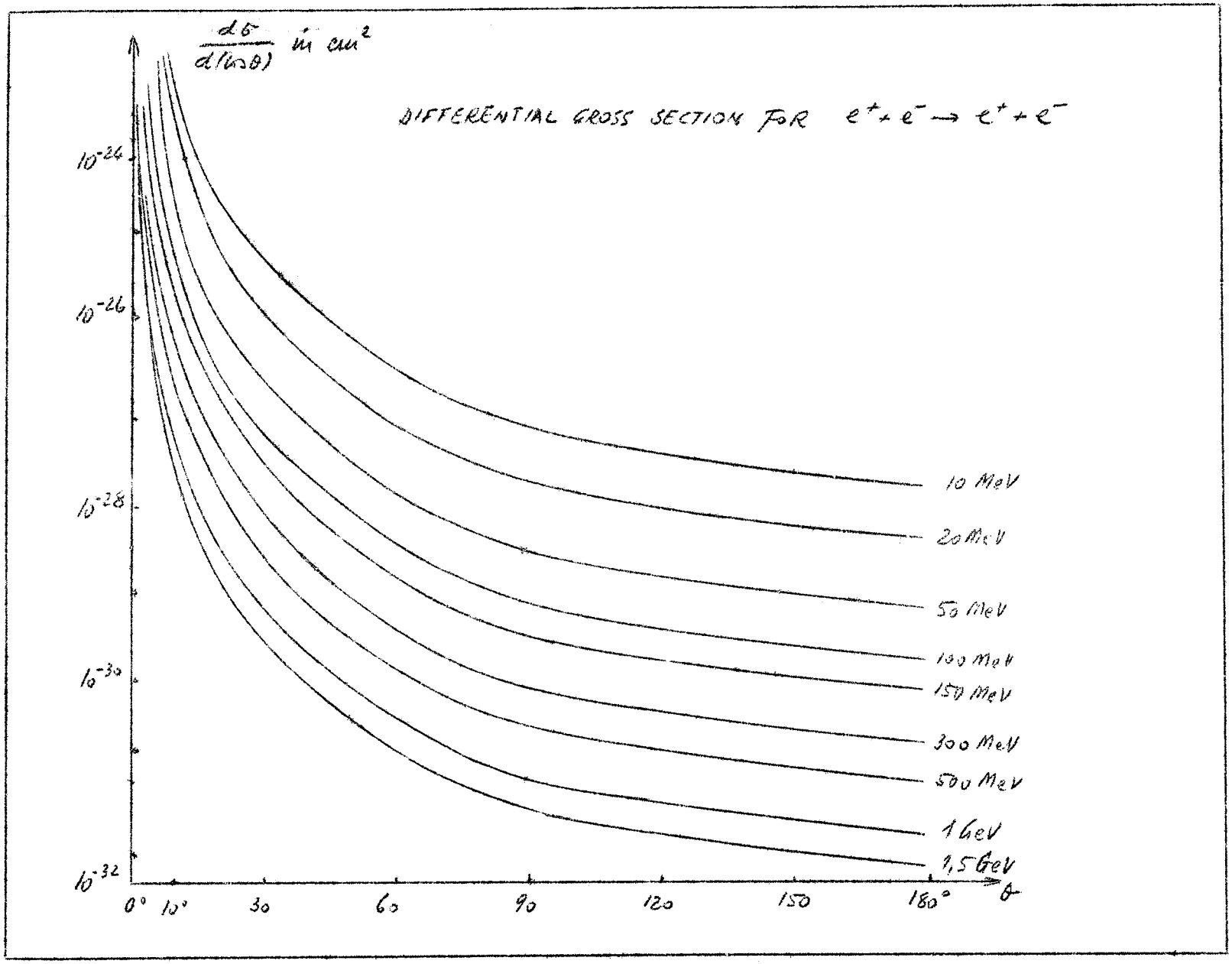
$\frac{d\sigma}{d(\cos\theta)}$ in cm²
DIFFERENTIAL CROSS SECTION FOR $e^+ + e^- \rightarrow e^+ + e^-$
10^{-24}
10^{-26}
10^{-28}
10^{-30}
10^{-32}
10 MeV
20 MeV
50 MeV
100 MeV
150 MeV
300 MeV
500 MeV
1 GeV
1,5 GeV
0° 10° 30 60 90 120 150 180° θ

FIG, 5

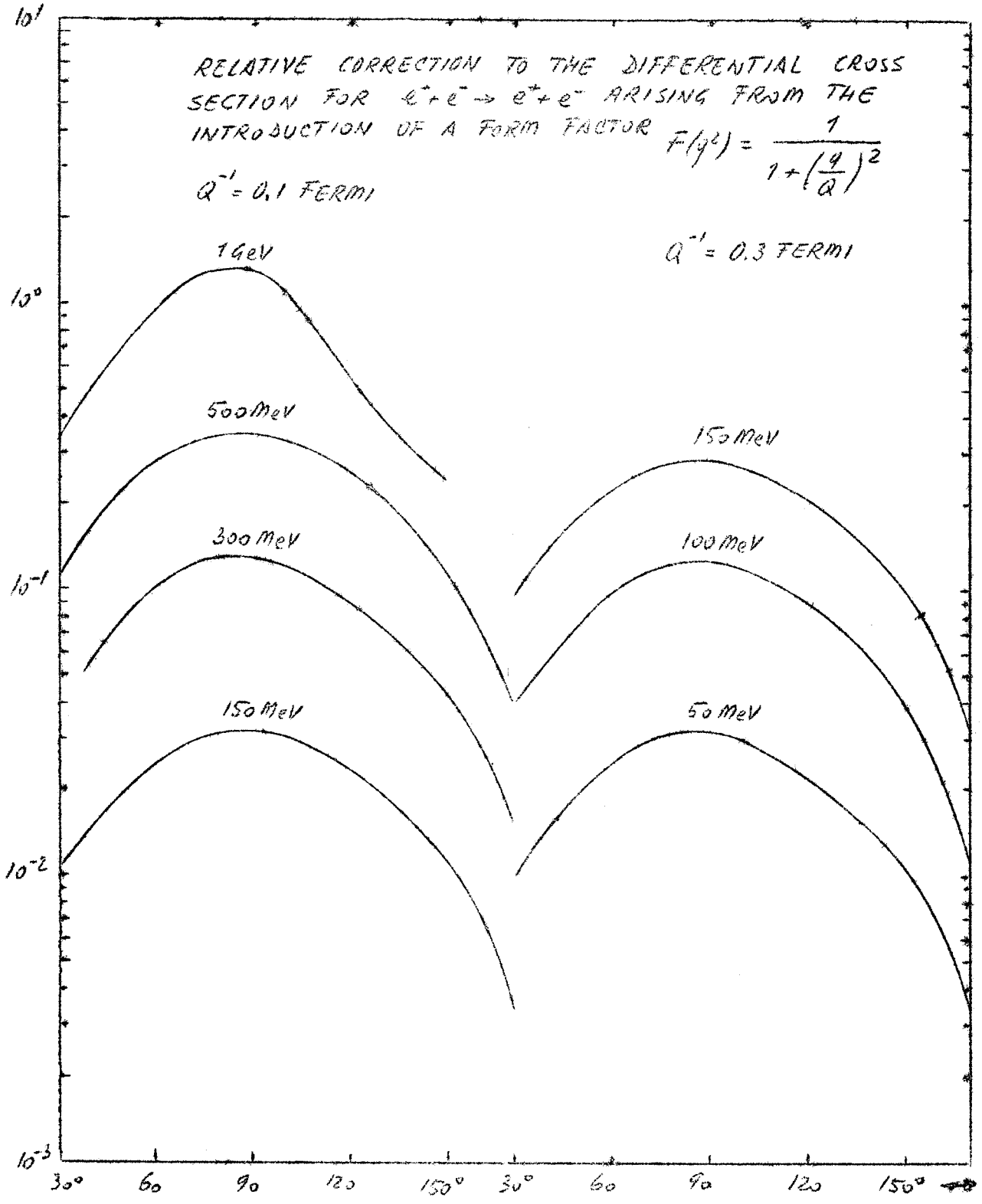
RELATIVE CORRECTION TO THE DIFFERENTIAL CROSS SECTION FOR $e^+ + e^- \rightarrow e^+ + e^-$ ARISING FROM THE INTRODUCTION OF A FORM FACTOR $F(q^2) = \frac{1}{1+\left(\frac{q}{Q}\right)^2}$
$Q^{-1} = 0.1$ FERMI
$Q^{-1} = 0.3$ FERMI
1 GeV
500 MeV
300 MeV
150 MeV
150 MeV
100 MeV
50 MeV
10^1
10^0
10^{-1}
10^{-2}
10^{-3}
30°
60
90
120
150°
30°
60
90
120
150°

FIG. 6

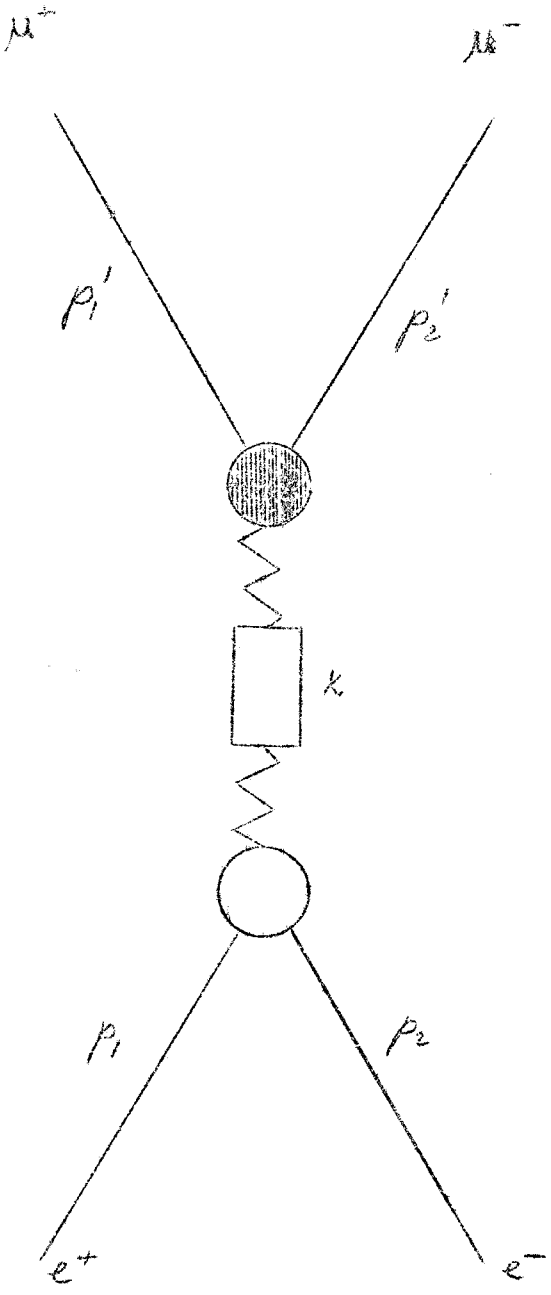

FIG. 7

DIFFERENTIAL CROSS SECTION FOR $e^+ + e^- \longrightarrow \mu^+ + \mu^-$

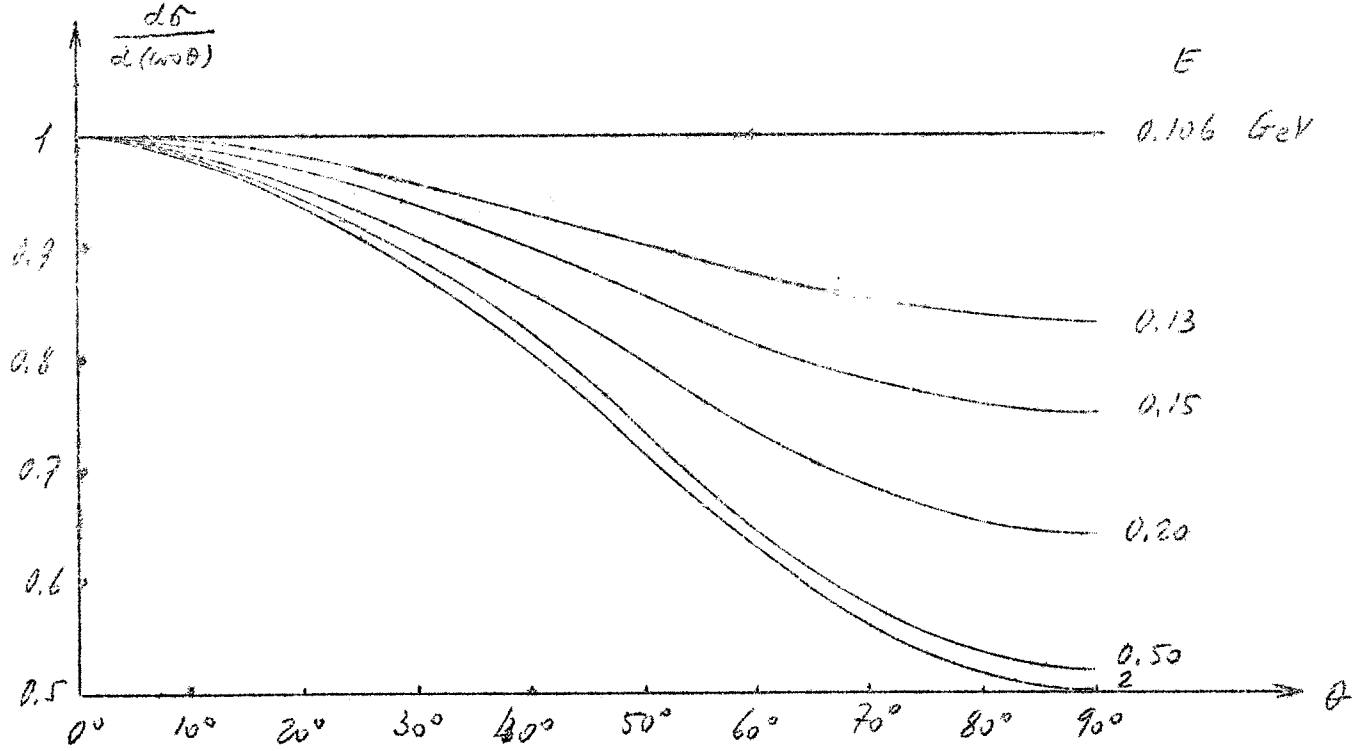

FIG. 8

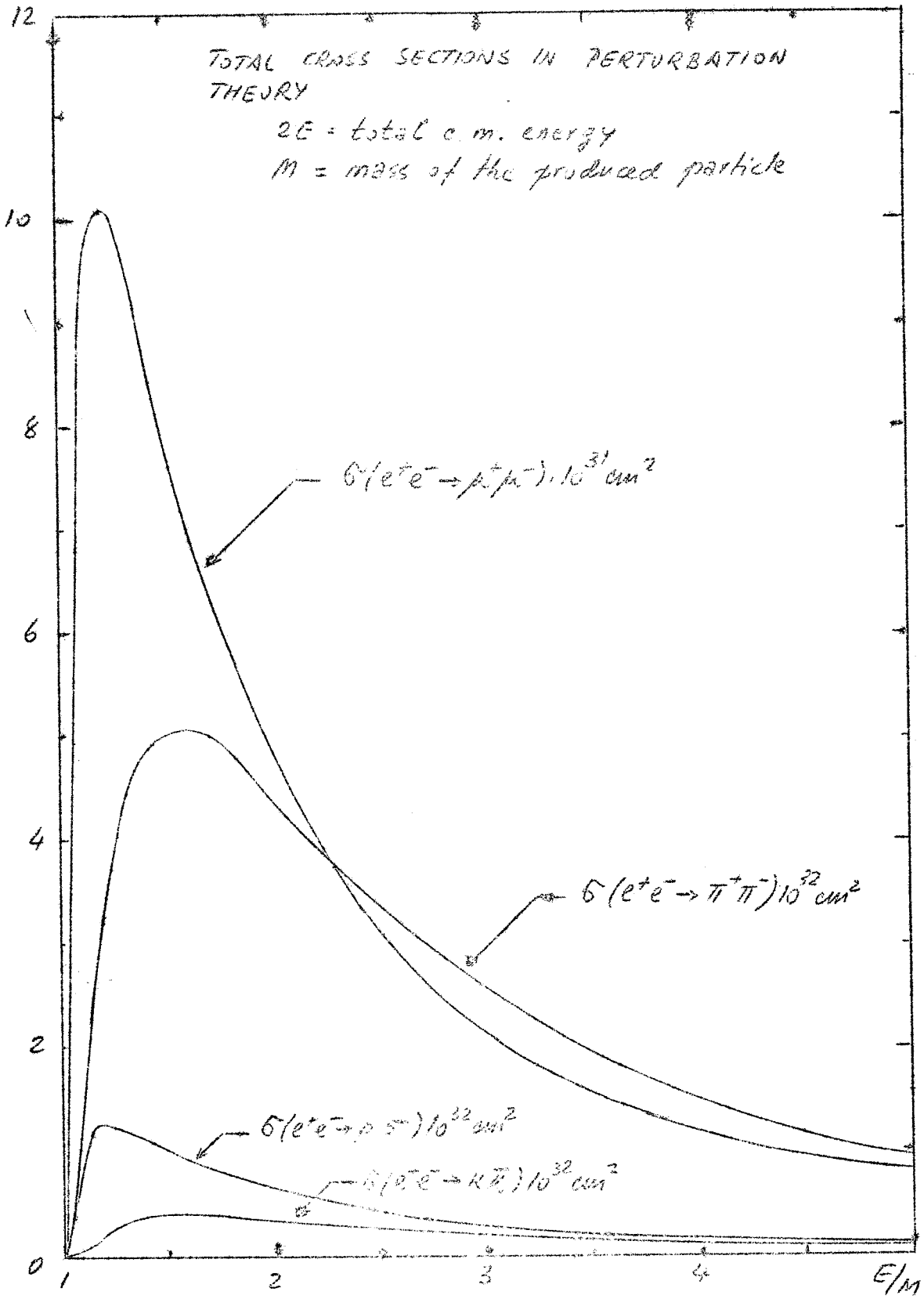
TOTAL CROSS SECTIONS IN PERTURBATION THEORY
2E = total c. m. energy
m = mass of the produced particle
12
10
8
6
4
2
0
1
2
3
4
E/m
σ(e⁺e⁻ → μ⁺μ⁻)·10³¹ cm²
σ(e⁺e⁻ → π⁺π⁻)10³² cm²
σ(e⁺e⁻ → ρ π⁻)10³² cm²
σ(e⁺e⁻ → K K̄)10³² cm²

FIG. 9

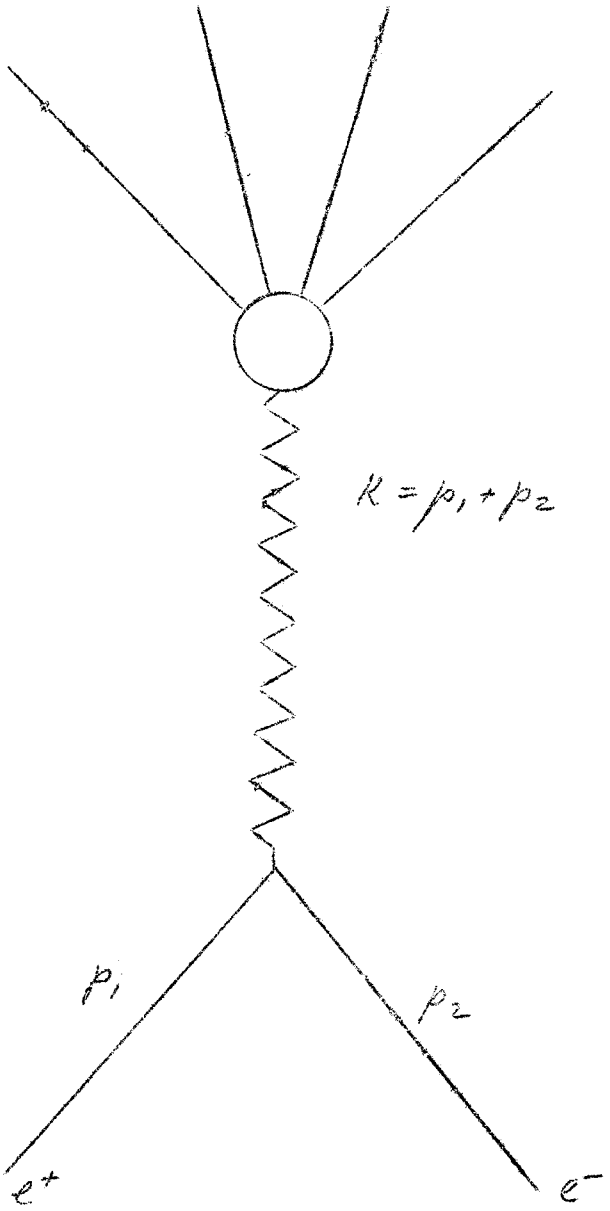

FIG. 10

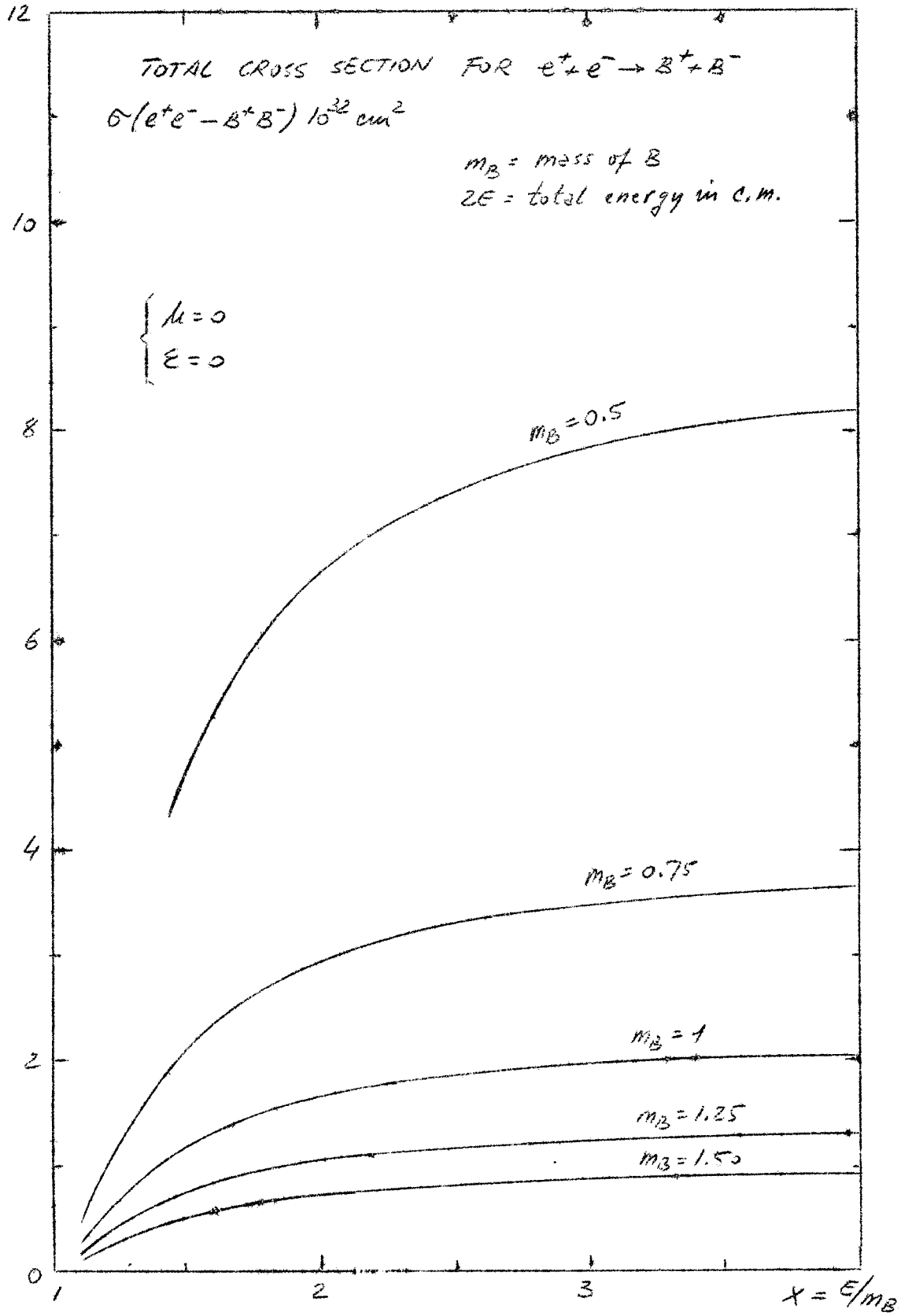
TOTAL CROSS SECTION FOR $e^+ + e^- \to B^+ + B^-$
$\sigma(e^+e^- - B^+B^-)\ 10^{22}\ cm^2$
m_B = mass of B
$2E$ = total energy in c.m.
$\mu = 0$
$\epsilon = 0$
$m_B = 0.5$
$m_B = 0.75$
$m_B = 1$
$m_B = 1.25$
$m_B = 1.50$
12
10
8
6
4
2
0
1
2
3
$x = E/m_B$

FIG. 11

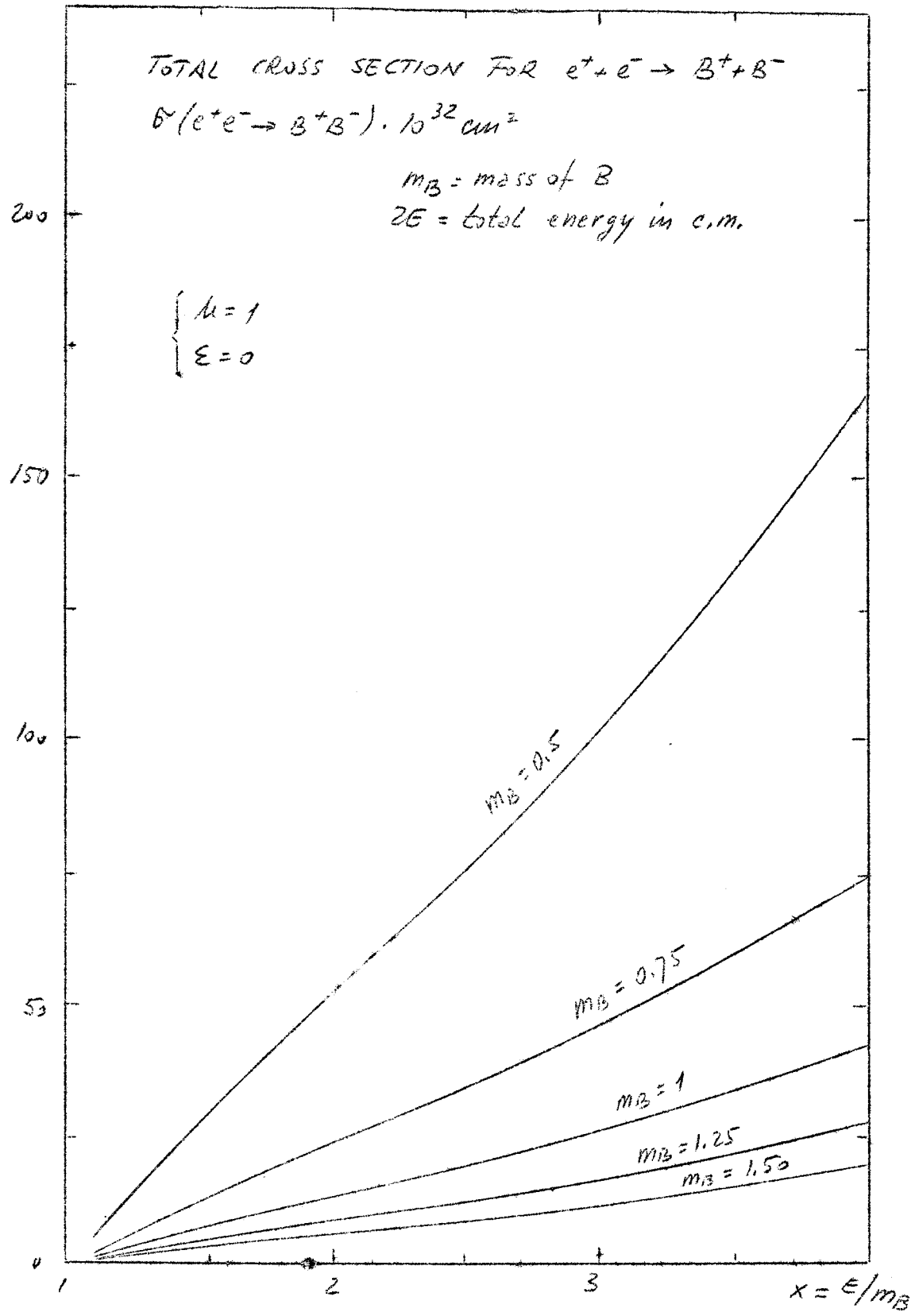
TOTAL CROSS SECTION FOR $e^+ + e^- \to B^+ + B^-$
$\sigma(e^+e^- \to B^+B^-) \cdot 10^{32}\ cm^2$
m_B = mass of B
2E = total energy in c.m.
$\mu = 1$
$\varepsilon = 0$
200
150
100
50
0
1
2
3
$x = E/m_B$
$m_B = 0.5$
$m_B = 0.75$
$m_B = 1$
$m_B = 1.25$
$m_B = 1.50$

FIG. 12

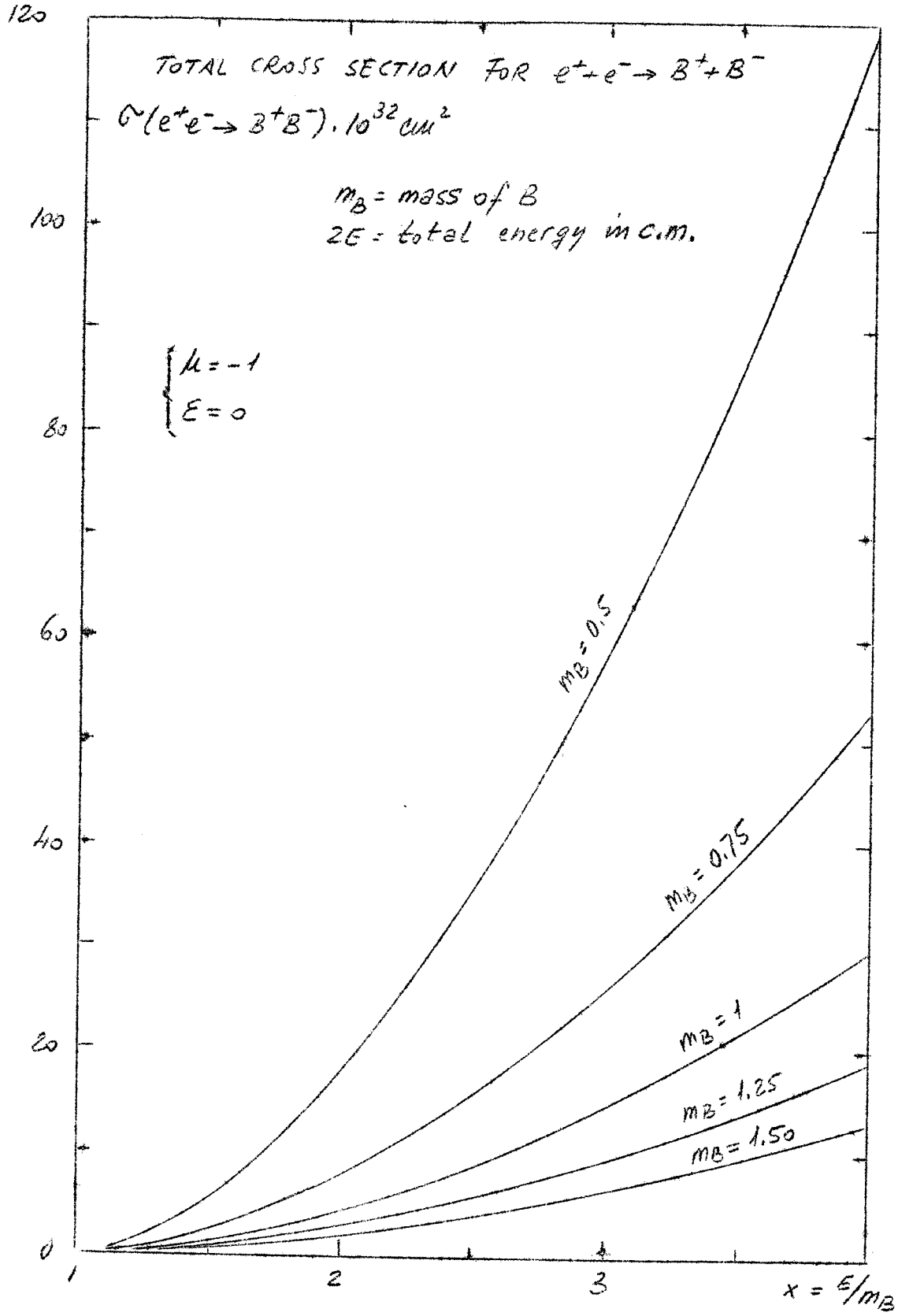
TOTAL CROSS SECTION FOR $e^+ + e^- \to B^+ + B^-$
$\sigma(e^+e^- \to B^+B^-) \cdot 10^{32}\ cm^2$
m_B = mass of B
2E = total energy in c.m.
$\mu = -1$
$\mathcal{E} = 0$
$m_B = 0.5$
$m_B = 0.75$
$m_B = 1$
$m_B = 1.25$
$m_B = 1.50$
120
100
80
60
40
20
0
1
2
3
$x = E/m_B$

FIG 13

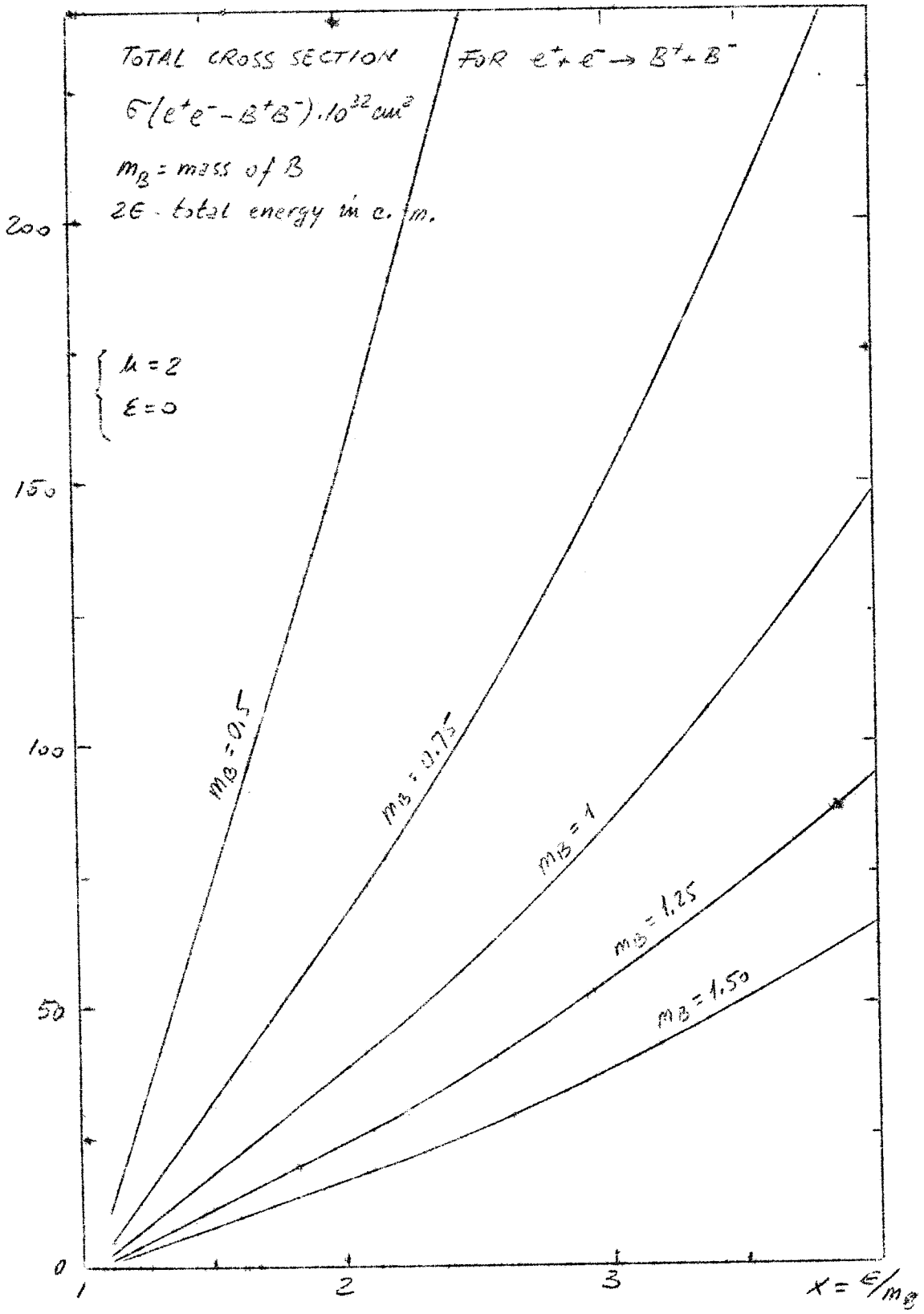
TOTAL CROSS SECTION FOR $e^+ + e^- \to B^+ + B^-$
$\sigma(e^+e^- - B^+B^-) \cdot 10^{32}\,cm^2$
m_B = mass of B
2E - total energy in c. m.
$\begin{cases} \mu = 2 \\ \varepsilon = 0 \end{cases}$
200
150
100
50
0
1
2
3
$x = E/m_B$
$m_B = 0.5$
$m_B = 0.75$
$m_B = 1$
$m_B = 1.25$
$m_B = 1.50$

FIG. 14

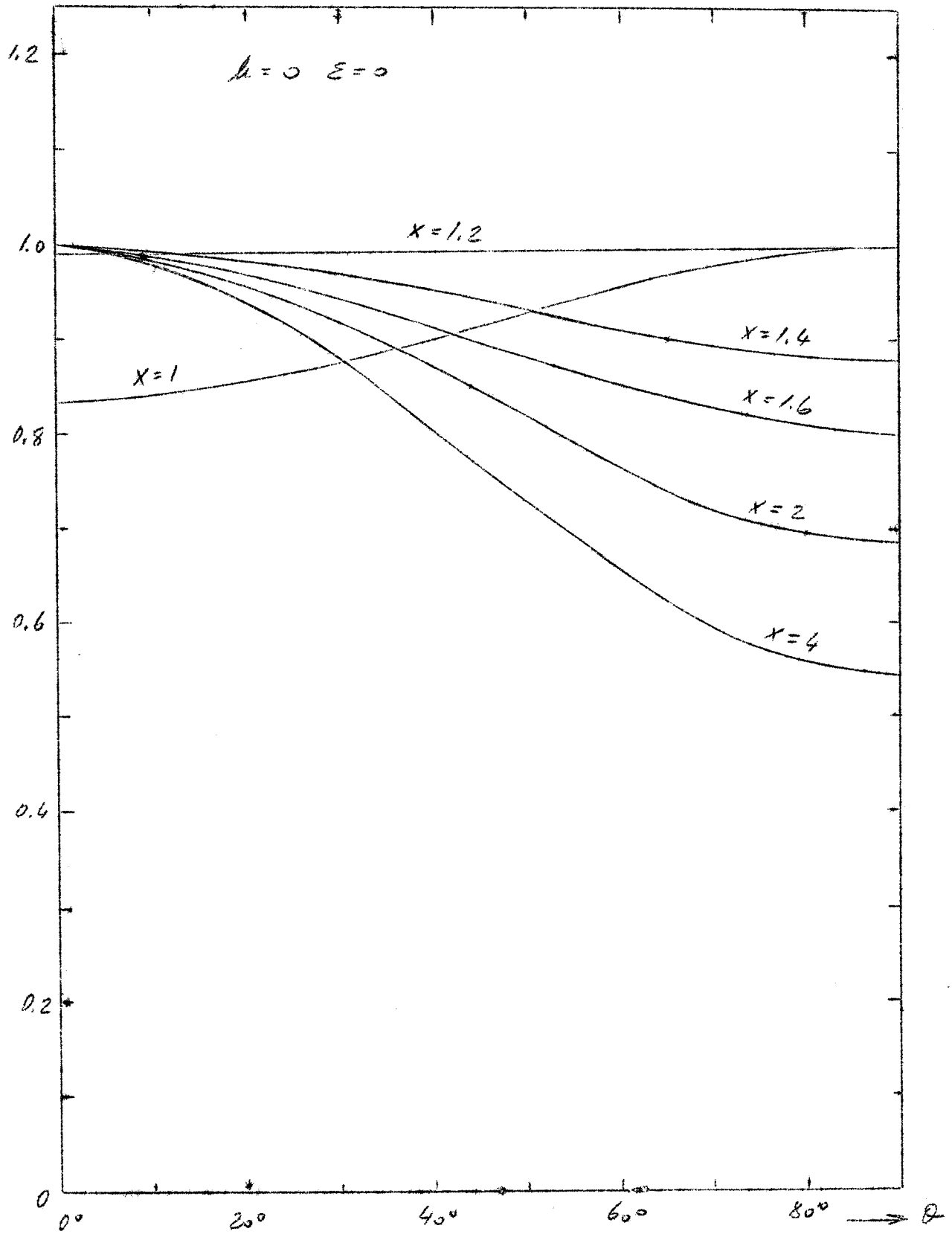

FIG. 15

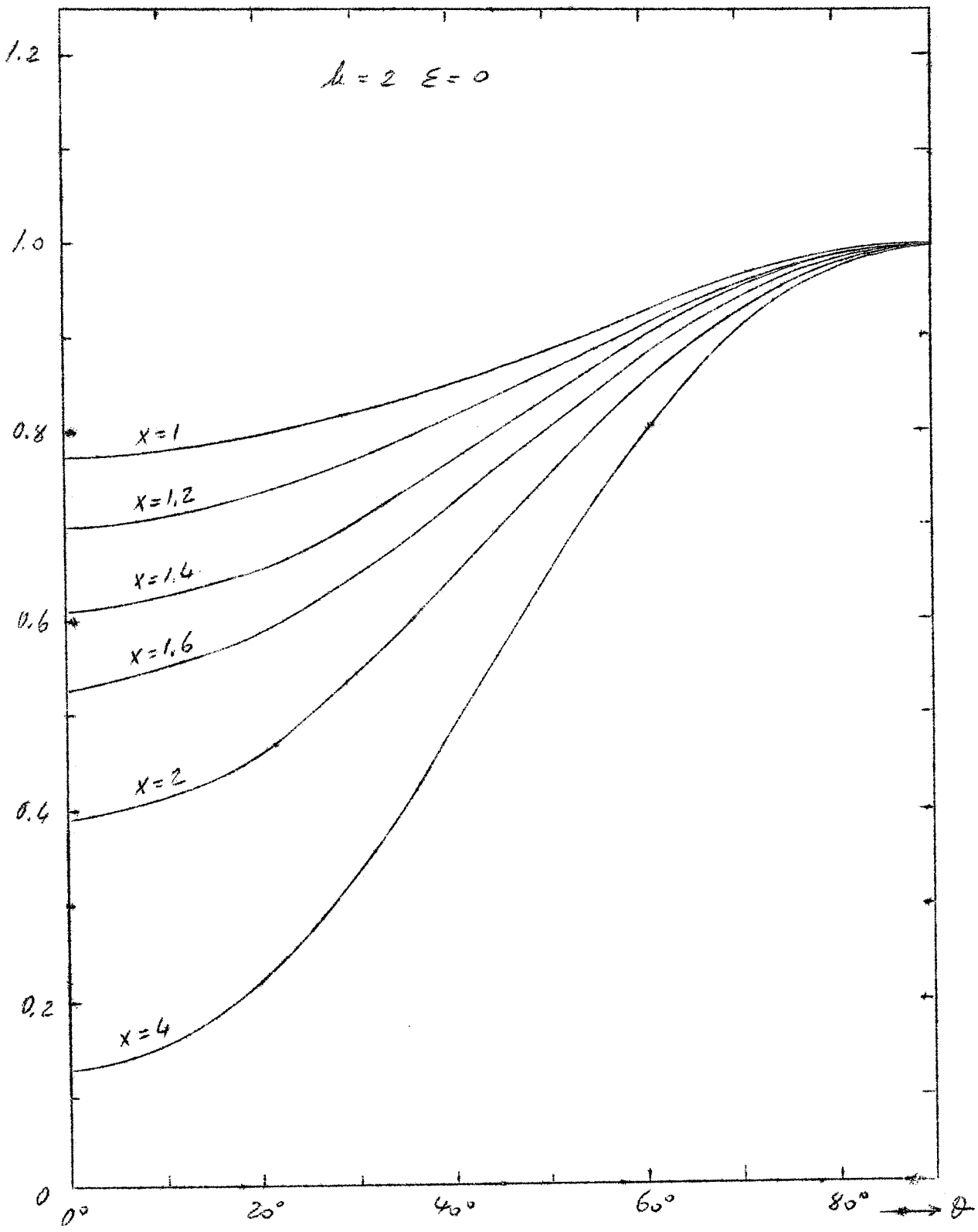
1.2
1.0
0.8
0.6
0.4
0.2
0
$\mu = 2 \quad \varepsilon = 0$
x = 1
x = 1.2
x = 1.4
x = 1.6
x = 2
x = 4
0°
20°
40°
60°
80°
θ

FIG. 16

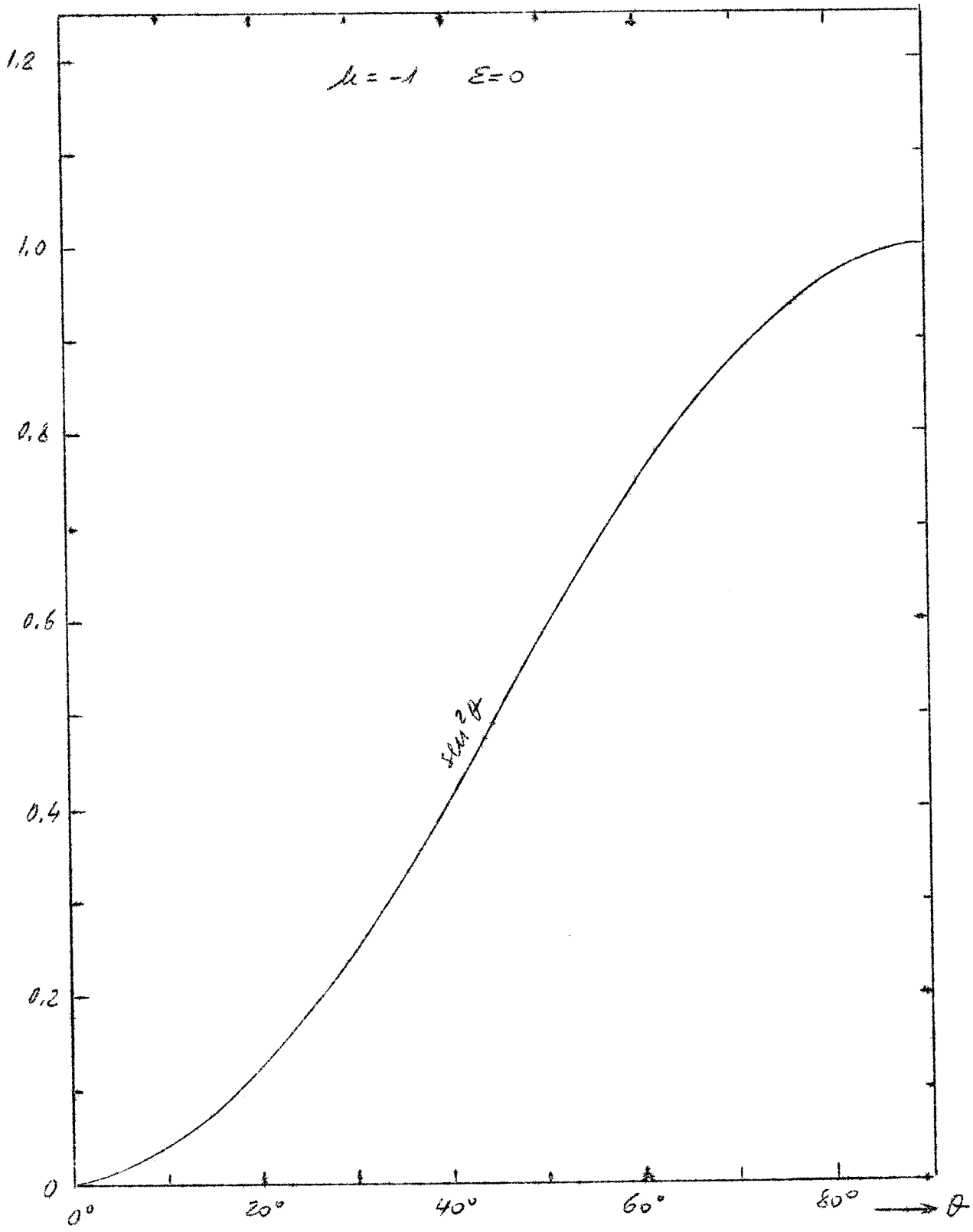

FIG. 17

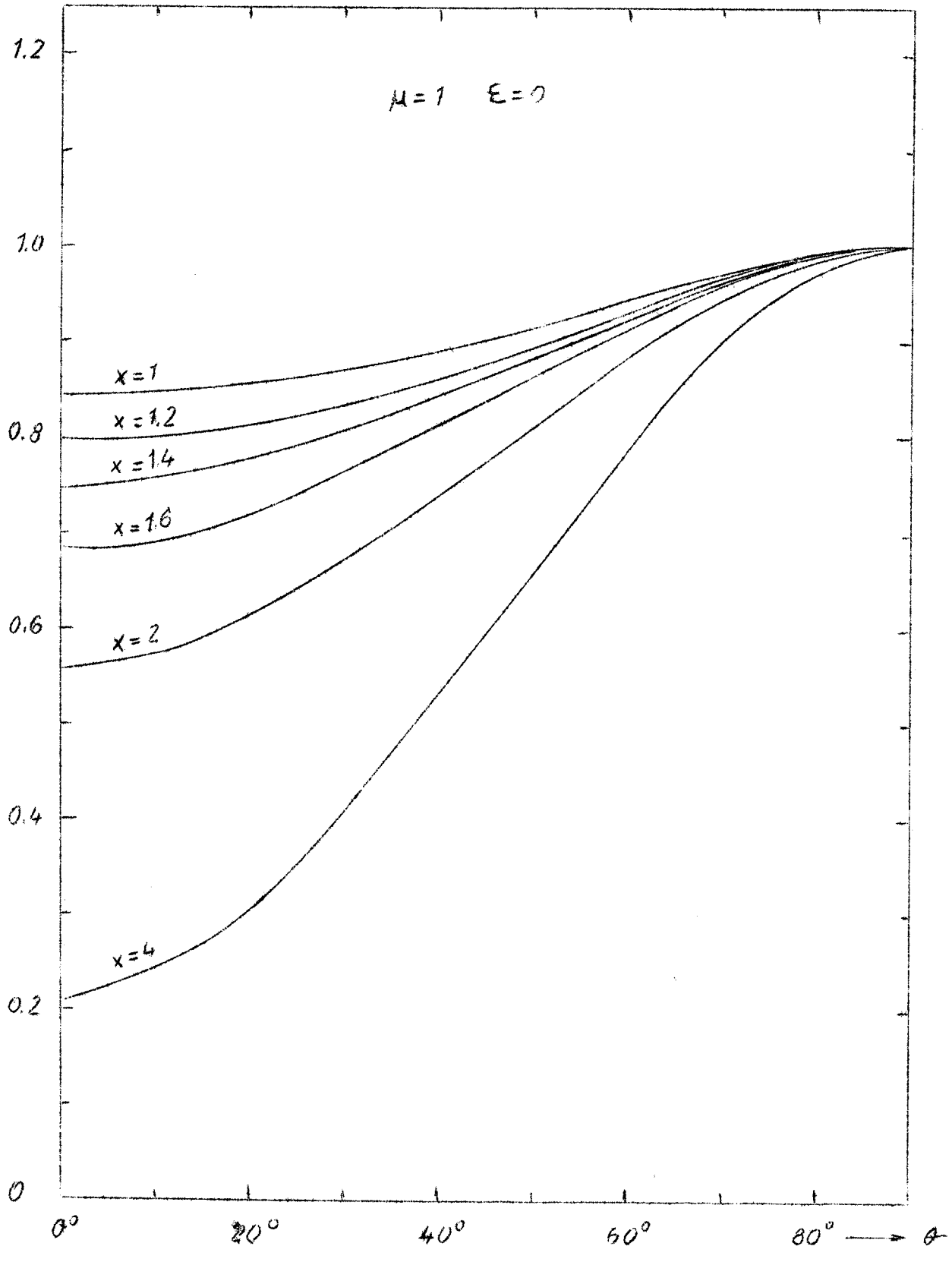

FIG. 18